ELECTRIC POWER
RESEARCH INSTITUTE

BWRVIP-111NP, Revision 1: BWR Vessel and Internals Project

Testing and Evaluation of BWR Supplemental Surveillance Program Capsules E, F, and I

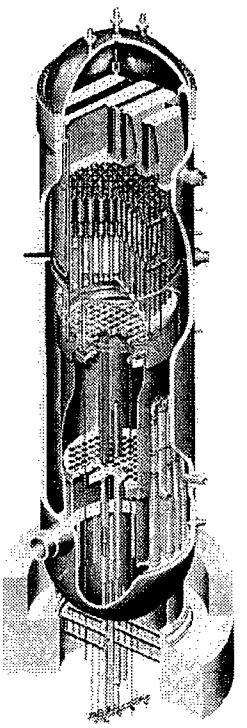

NON-PROPRIETARY INFORMATION

NOTICE: This report contains the non-propriety information that is included in the proprietary version of this report. The proprietary version of this report contains proprietary information that is the intellectual property of BWRVIP utility members and EPRI. Accordingly, the proprietary report is available only under license from EPRI and may not be reproduced or disclosed, wholly or in part, by any Licensee to any other person or organization.

BWRVIP-111NP, Revision 1: BWR Vessel and Internals Project

Testing and Evaluation of BWR Supplemental Surveillance Program Capsules E, F and I

1015001NP

Revised Report, September 2007

EPRI Project Manager
R. Carter

ELECTRIC POWER RESEARCH INSTITUTE
3420 Hillview Avenue, Palo Alto, California 94304-1338 • PO Box 10412, Palo Alto, California 94303-0813 • USA
800.313.3774 • 650.855.2121 • askepri@epri.com • www.epri.com

DISCLAIMER OF WARRANTIES AND LIMITATION OF LIABILITIES

THIS DOCUMENT WAS PREPARED BY THE ORGANIZATION(S) NAMED BELOW AS AN ACCOUNT OF WORK SPONSORED OR COSPONSORED BY THE BWR VESSEL AND INTERNALS PROJECT (BWRVIP) AND ELECTRIC POWER RESEARCH INSTITUTE, INC. (EPRI). NEITHER BWRVIP, EPRI, ANY MEMBER OF EPRI, ANY COSPONSOR, THE ORGANIZATION(S) BELOW, NOR ANY PERSON ACTING ON BEHALF OF ANY OF THEM:

(A) MAKES ANY WARRANTY OR REPRESENTATION WHATSOEVER, EXPRESS OR IMPLIED, (I) WITH RESPECT TO THE USE OF ANY INFORMATION, APPARATUS, METHOD, PROCESS, OR SIMILAR ITEM DISCLOSED IN THIS DOCUMENT, INCLUDING MERCHANTABILITY AND FITNESS FOR A PARTICULAR PURPOSE, OR (II) THAT SUCH USE DOES NOT INFRINGE ON OR INTERFERE WITH PRIVATELY OWNED RIGHTS, INCLUDING ANY PARTY'S INTELLECTUAL PROPERTY, OR (III) THAT THIS DOCUMENT IS SUITABLE TO ANY PARTICULAR USER'S CIRCUMSTANCE; OR

(B) ASSUMES RESPONSIBILITY FOR ANY DAMAGES OR OTHER LIABILITY WHATSOEVER (INCLUDING ANY CONSEQUENTIAL DAMAGES, EVEN IF BWRVIP, EPRI OR ANY EPRI REPRESENTATIVE HAS BEEN ADVISED OF THE POSSIBILITY OF SUCH DAMAGES) RESULTING FROM YOUR SELECTION OR USE OF THIS DOCUMENT OR ANY INFORMATION, APPARATUS, METHOD, PROCESS, OR SIMILAR ITEM DISCLOSED IN THIS DOCUMENT.

ORGANIZATION(S) THAT PREPARED THIS DOCUMENT

ATI Consulting

BWXT Services, Inc.

TransWare Enterprises Inc.

NON-PROPRIETARY INFORMATION

NOTICE: This report contains the non-propriety information that is included in the proprietary version of this report. The proprietary version of this report contains proprietary information that is the intellectual property of BWRVIP utility members and EPRI. Accordingly, the proprietary report is available only under license from EPRI and may not be reproduced or disclosed, wholly or in part, by any Licensee to any other person or organization.

NOTE

For further information about EPRI, call the EPRI Customer Assistance Center at 800.313.3774 or e-mail askepri@epri.com.

Electric Power Research Institute, EPRI, and TOGETHER...SHAPING THE FUTURE OF ELECTRICITY are registered service marks of the Electric Power Research Institute, Inc.

Copyright © 2007 Electric Power Research Institute, Inc. All rights reserved.

CITATIONS

This report was prepared by

ATI Consulting
P.O. Box 5769
Pinehurst, NC 28374

Principal Investigators
T. Hardin
B. Burgos

BWX Technologies, Inc.
2016 Mt. Athos Road
Lynchburg, VA 24504

Principal Investigator
K. Hour

TransWare Enterprises Inc.
1565 Mediterranean Drive
Suite A
Sycamore, IL 60178

Principal Investigators
C. Potze
K. Watkins

This report describes research sponsored by the Electric Power Research Institute (EPRI) and its BWRVIP participating members.

The report is a corporate document that should be cited in the literature in the following manner:

BWRVIP-111NP, Revision 1: BWR Vessel and Internals Project Testing and Evaluation of BWR Supplemental Surveillance Program Capsules E, F and I. EPRI, Palo Alto, CA: 2007. 1015001NP.

This report is based on the following previously published report:

BWRVIP-111: BWR Vessel and Internals Project, Testing and Evaluation of BWR Supplemental Surveillance Program Capsules E, F and I, EPRI, Palo Alto, CA: 2002. 1003553 authored by ATI Consulting principal investigator B. Burgos, BWXT Services, Inc. principal investigator K. Hour, and TransWare Enterprises Inc. principal investigators C. Potze and K. Watkins.

REPORT SUMMARY

Each boiling water reactor (BWR) has a surveillance program for monitoring changes in reactor pressure vessel (RPV) material properties due to neutron irradiation. This report describes testing and evaluation of BWR Supplemental Surveillance Program (SSP) capsules E, F and I. These results will be used to monitor embrittlement as part of the BWR Vessel and Internals Project (BWRVIP) Integrated Surveillance Program (ISP).

Results & Findings

The report includes specimen chemical compositions, capsule neutron exposure, specimen temperatures during irradiation and Charpy V-notch test results. Photographs of the Charpy specimen fracture surfaces are also provided. The project compared irradiated Charpy data for the specimens to unirradiated data to determine the shift in Charpy curves due to irradiation. Results indicate a shift lower than the predictions of Regulatory Guide 1.99, Revision 2, for all but two of the materials. Upper shelf energy results indicate a larger decrease than the predictions from Regulatory Guide 1.99, Revision 2, for eighteen of the thirty materials. Flux wires were measured and fluence was determined for each specimen set within the three capsules. Fluence values were somewhat higher than the original target values due to an extension in the operating cycle at Oyster Creek from 18 to 24 months.

Challenges & Objectives

Neutron irradiation exposure reduces the toughness of reactor vessel steel plates, welds and forgings. The objectives of this project were twofold:

- To document results of the neutron dosimetry and Charpy-V notch ductility tests for materials contained in the SSP capsules E, F and I.
- To compare results with the embrittlement trend prediction of U.S. Nuclear Regulatory Commission (USNRC) Regulatory Guide 1.99, Revision 2.

Applications, Values & Use

Results of this work will be used in the BWRVIP ISP that will integrate individual BWR surveillance programs into a single program. Data generated from the SSP specimens will provide significant additional data of high quality to monitor BWR vessel embrittlement. The ISP and the use of the SSP capsule specimen data will result in significant cost savings to the BWR fleet and provide more accurate monitoring of embrittlement in BWRs.

EPRI Perspective

The BWRVIP ISP represents a major enhancement to the process of monitoring embrittlement for the U.S. fleet of BWRs. The ISP optimizes surveillance capsule tests while at the same time maximizing the quantity and quality of data, thus resulting in a more cost-effective program. The BWRVIP ISP will provide more representative data that may be used to assess embrittlement in RPV vessel beltline materials and improve trend curves in the BWR range of irradiation conditions.

Approach

The capsules were inserted into the Oyster Creek reactor in February 1993 at a location of sufficient lead factor to provide the desired fluence. In October 2000, the capsules were removed from the reactor and transported to facilities for testing and evaluation. Dosimetry was used to gather information about the neutron fluence accrual of the specimens and thermal monitors were placed in the capsule to approximate the highest temperature during irradiation. A neutron transport calculation was performed in accordance with Regulatory Guide 1.190 and compared to the results from the dosimetry. Testing of Charpy V-notch specimens were performed according to ASTM standards.

Keywords

Reactor pressure vessel integrity
Reactor vessel surveillance program
Radiation embrittlement
BWR
Charpy testing
Mechanical properties

ABSTRACT

This report describes the testing and evaluation of BWR Supplemental Surveillance Program (SSP) capsules E, F and I. These capsules were installed in the Oyster Creek reactor in February 1993 and removed in October 2000. The capsules contained flux wires for neutron fluence measurement, thermal monitors to measure temperature and Charpy test specimens for material property evaluations. The flux wires were evaluated to determine the fluence experienced by the test specimens. Thermal monitors were evaluated to determine the maximum temperature experienced by the specimens. Charpy V-notch impact testing was performed to establish the mechanical properties of the irradiated surveillance materials.

RECORD OF REVISIONS

Revision Number	Revisions
BWRVIP-111	Original Report (1003553).
Revision 1	The report as originally published (1003553) was revised to incorporate changes to the best estimate chemistry values and baseline (unirradiated) Charpy V-notch reference temperatures of some materials to reflect additional testing and analyses conducted since this report was first published. For those materials with changes, shifts, predicted shifts, USE drops and predicted USE drops were recalculated as required. Other editorial changes, clarifications and corrections for typographical errors were made as required. Minor changes (e.g., 0.1°F) were made to the shift predictions for some materials due to a more precise, refreshed calculation. Details of the revision can be found in Appendix E.

CONTENTS

1 INTRODUCTION 1-1

Implementation Requirements 1-1

2 MATERIALS 2-1

Chemical Compositions 2-1

Material Description 2-4

Unirradiated Properties 2-6

CVN Baseline Properties 2-6

3 TEST SPECIMEN DESCRIPTION 3-1

Charpy V-Notch Specimens 3-2

Dosimeters 3-3

Thermal Monitors 3-4

4 MATERIAL IRRADIATION 4-1

Reactor System Geometry and SSP Surveillance Capsules 4-1

Reactor System Material Compositions 4-6

Core Region Materials 4-6

Ex-Core Region Materials 4-6

Reactor Operating Data 4-8

Plant Power History 4-8

Cycle State Point Data 4-8

Core Loading Pattern 4-12

Calculation Methodology 4-13

Three-Dimensional Flux Synthesis 4-13

Planar (Rθ) Flux Solution Model 4-14

Axi-Symmetric (RZ) Flux Solution Mode 4-16

Radial (R) Flux Solution Model 4-17

Neutron Source Generation 4-17
Peripheral Assembly Pin Powers 4-18
Surveillance Capsule Flux Perturbation Calculation 4-21
Nuclear Data Library 4-24
Nuclear Cross Sections 4-24
Activation Response Functions 4-30
Fluence Evaluation Results 4-32
Surveillance Capsule Evaluation 4-33
Comparison of Predicted Activation to Measurements 4-33
Surveillance Capsule Calculated Neutron Fluence and Flux 4-37
Surveillance Capsule Best Estimate Neutron Fluence and Flux 4-40

5 RESULTS 5-1
Charpy V-Notch Testing 5-1
Impact Test Procedure 5-1
Impact Test Results 5-2
Analysis of Impact Test Results 5-2
Irradiated Versus Unirradiated CVN Properties 5-2
Discussion 5-18

6 REFERENCES 6-1

A SUMMARY OF CHARPY V-NOTCH TEST DATA A-1

B TANH CURVE FIT PLOTS OF CVN TEST DATA B-1

C CVN FRACTURE APPEARANCE PHOTOGRAPHS C-1

D DOSIMETER ANALYSIS D-1
Quantitative Gamma Spectrometry D-1
Geometry Corrections for Wire and Foil Type Dosimeters D-1
Wire Type Dosimeters D-2
Foil Type Dosimeters D-3
Attenuation Corrections for Wire and Foil Type Dosimeters D-4
Wire Type Dosimeter D-4
Foil Type Dosimeter D-5

Dosimeter Specific Activities D-6
References D-10

***E* RECORD OF REVISIONS E-1**

LIST OF FIGURES

Figure 4-1 Oyster Creek Core Configuration 4-2
Figure 4-2 Oyster Creek SSP Capsule Holder 4-4
Figure 4-3 Capsules E and F Description 4-5
Figure 4-4 Capsule I Description 4-5
Figure 4-5 DORT Rθ Octant Model of Oyster Creek Reactor 4-14
Figure 4-6 Radial Zone Assignement Assemblies in a Core Octant 4-15
Figure 4-7 Orientation of Peripheral Assembly Types in a Core Octant 4-19
Figure D-1 Wire on PetriSlide™ D-3
Figure D-2 Foil on PetriSlide™ D-4

LIST OF TABLES

Table 2-1 Materials Irradiated in SSP (Oyster Creek) Capsule E 2-2
Table 2-2 Materials Irradiated in SSP (Oyster Creek) Capsule F 2-3
Table 2-3 Materials Irradiated in SSP (Oyster Creek) Capsule I 2-4
Table 2-4 Plate Materials Irradiated in SSP (Oyster Creek) Capsules E, F and I 2-5
Table 2-5 Weld Materials Irradiated in SSP (Oyster Creek) Capsules E, F and I 2-5
Table 2-6 Baseline CVN Properties of SSP (Oyster Creek) Capsule E 2-6
Table 2-7 Baseline CVN Properties of SSP (Oyster Creek) Capsule F 2-7
Table 2-8 Baseline CVN Properties of SSP (Oyster Creek) Capsule I 2-8
Table 3-1 Quantities of Specimens in SSP (Oyster Creek) Capsules E, F and I 3-1
Table 3-2 Additional Special Dosimetry in SSP (Oyster Creek) Capsules E, F and I 3-4
Table 3-3 Thermal Monitors Contained in SSP (Oyster Creek) Capsule I 3-5
Table 4-1 Oyster Creek Reactor System Design Data 4-3
Table 4-2 Saturated Water at In-core Operating Conditions 4-6
Table 4-3 Material Composition of the Shroud 4-7
Table 4-4 Material Composition of the Reactor Pressure Vessel 4-7
Table 4-5 Material Composition of the Biological Shield Wall 4-7
Table 4-6 Material Composition of the Core Support Plate Region 4-7
Table 4-7 Material Composition of the Top Guide Region 4-8
Table 4-8 Cycle 14 Operating State Points 4-9
Table 4-9 Cycle 15 Operating State Points 4-10
Table 4-10 Cycle 16 Operating State Points 4-11
Table 4-11 Cycle 17 Operating State Points 4-12
Table 4-12 Summary of Oyster Creek Core Loading Pattern 4-13
Table 4-13 Pin Powers for Eight by Eight Array for Type 1 (Peripheral Side) Assemblies 4-19
Table 4-14 Pin Powers for Eight by Eight Array for Type 2 (Peripheral Corner) Assemblies 4-20
Table 4-15 Pin Powers for Eight by Eight Array for Type 3 (2nd Row Side) Assemblies 4-20
Table 4-16 Pin Powers for Eight by Eight Array for Type 4 (2nd Row Corner) Assemblies 4-20
Table 4-17 Capsule Flux Multiplication Factors for Cycles 14 and 15 4-22
Table 4-18 Capsule Flux Multiplication Factors for Cycles 16 and 17 4-23
Table 4-19 BUGLE-96 Neutron Energy Group Structure (Neutron Cross Section Set) 4-25
Table 4-20 BUGLE-96 Gamma Energy Group Structure (Photon Cross Section Set) 4-26

Table 4-21 List of BUGLE 96 Nuclides 4-27
Table 4-22 Row Positions of Response Functions in BUGLE-96 Tables 7001 and 7003 4-31
Table 4-23 Row Positions of Response Functions in BUGLE-96 Tables 7002 and 7004 4-32
Table 4-24 Capsule E Iron Flux Wire Comparison 4-33
Table 4-25 Capsule E Copper Flux Wire Comparison 4-34
Table 4-26 Capsule E Dosimetry Comparison 4-34
Table 4-27 Capsule F Iron Flux Wire Comparison 4-35
Table 4-28 Capsule F Copper Flux Wire Comparison 4-35
Table 4-29 Capsule I Iron Flux Wire Comparison 4-36
Table 4-30 Capsule I Copper Flux Wire Comparison 4-36
Table 4-31 Capsule I Dosimetry Comparison 4-37
Table 4-32 Calculated Neutron Fluence and Rated Power Flux for Energy > 1 MeV in Capsule E 4-38
Table 4-33 Calculated Neutron Fluence and Rated Power Flux for Energy > 0.1 MeV in Capsule E 4-38
Table 4-34 Calculated Neutron Fluence and Rated Power Flux for Energy > 1 MeV in Capsule F 4-39
Table 4-35 Calculated Neutron Fluence and Rated Power Flux for Energy > 0.1 MeV in Capsule F 4-39
Table 4-36 Calculated Neutron Fluence and Rated Power Flux for Energy > 1 MeV in Capsule I 4-40
Table 4-37 Calculated Neutron Fluence and Rated Power Flux for Energy > 0.1 MeV in Capsule I 4-40
Table 4-38 Best Estimate Neutron Fluence and Rated Power Flux for Energy > 1 MeV in Capsule E 4-41
Table 4-39 Best Estimate Neutron Fluence and Rated Power Flux for Energy > 0.1 MeV in Capsule E 4-41
Table 4-40 Best Estimate Neutron Fluence and Rated Power Flux for Energy > 1 MeV in Capsule F 4-42
Table 4-41 Best Estimate Neutron Fluence and Rated Power Flux for Energy > 0.1 MeV in Capsule F 4-42
Table 4-42 Best Estimate Neutron Fluence and Rated Power Flux for Energy > 1 MeV in Capsule I 4-43
Table 4-43 Best Estimate Neutron Fluence and Rated Power Flux for Energy > 0.1 MeV in Capsule I 4-43
Table 5-1 Effect of Irradiation (E>1.0 MeV) on the Notch Toughness Properties of Capsule E Materials 5-3
Table 5-2 Effect of Irradiation (E>1.0 MeV) on the Notch Toughness Properties of Capsule F Materials 5-5
Table 5-3 Effect of Irradiation (E>1.0 MeV) on the Notch Toughness Properties of Capsule I Materials 5-7

Table 5-4 Effect of Irradiation (E>1.0 MeV) on the Notch Toughness Properties of Capsule E and I EP2 Plate Materials[1] 5-9
Table 5-5 Effect of Irradiation (E>1.0 MeV) on the Notch Toughness Properties of Capsule E and I A1224-1 Grand Gulf Plate Materials 5-10
Table 5-6 Effect of Irradiation (E>1.0 MeV) on the Notch Toughness Properties of Capsule E and I C2331-2 Cooper Plate Materials 5-11
Table 5-7 Effect of Irradiation (E>1.0 MeV) on the Notch Toughness Properties of Capsule E and I P2130-2 Nine Mile Point 1 Plate Materials 5-12
Table 5-8 Effect of Irradiation (E>1.0 MeV) on the Notch Toughness Properties of Capsule E and I C3278-2 FitzPatrick Plate Materials 5-13
Table 5-9 Effect of Irradiation (E>1.0 MeV) on the Notch Toughness Properties of Capsule E and I 5P6214B Grand Gulf Weld Materials 5-14
Table 5-10 Effect of Irradiation (E>1.0 MeV) on the Notch Toughness Properties of Capsule E and I 34B009 Millstone 1 Weld Materials 5-15
Table 5-11 Effect of Irradiation (E>1.0 MeV) on the Notch Toughness Properties of Capsule E and I EP2-21 and IP2-21 (QC2 ESW) Weld Materials 5-16
Table 5-12 Effect of Irradiation (E>1.0 MeV) on the Notch Toughness Properties of Capsule E and I 406L44 Quad Cities 1 Weld Materials 5-17
Table 5-13 Comparison of Actual Versus Predicted Embrittlement of SSP (Oyster Creek) Capsule E Materials 5-19
Table 5-14 Comparison of Actual Versus Predicted Embrittlement of SSP (Oyster Creek) Capsule F Materials 5-20
Table 5-15 Comparison of Actual Versus Predicted Embrittlement of SSP (Oyster Creek) Capsule I Materials 5-21
Table 5-16 Comparison of Actual Versus Predicted Percent Decrease in Upper Shelf Energy (USE) of SSP (Oyster Creek) Capsule E Materials 5-22
Table 5-17 Comparison of Actual Versus Predicted Percent Decrease in Upper Shelf Energy (USE) of SSP (Oyster Creek) Capsule F Materials 5-23
Table 5-18 Comparison of Actual Versus Predicted Percent Decrease in Upper Shelf Energy (USE) of SSP (Oyster Creek) Capsule I Materials 5-24
Table D-1 Table of Quantifying Gamma Rays D-1
Table D-2 Isotopic Fractions and Weight Fractions of Target Nuclides D-6
Table D-3 Specific Activities of BWR VIP Capsules E/F and I Dosimetry D-7
Table E-1 Revision Details E-2

1
INTRODUCTION

Part of the effort to assure reactor vessel integrity involves evaluation of the fracture toughness of the vessel ferritic materials. The key values that characterize fracture toughness are the reference temperature of nil-ductility transition (RT_{NDT}) and the upper shelf energy (USE). These are defined in 10CFR50 Appendix G [1] and in Appendix G of the ASME Boiler and Pressure Vessel Code, Section XI [2]. Appendix H of 10CFR50 [1] and ASTM E185-82 [3] establish the methods to be used for testing of the Supplemental Surveillance Program (SSP) test materials.

Nine (9) capsules containing test specimens were placed in two host reactors as part of the SSP. Three capsules (designated A, B and C) were placed into the Cooper reactor and the remaining six capsules (designated D through I) were placed into the Oyster Creek reactor. The results from the first set of capsules (Capsules D, G and H) have been reported in EPRI 1000890 [4]. This report addresses the second set of capsules (Capsules E, F and I) of the SSP removed and tested under this program. These capsules were irradiated at the Oyster Creek Nuclear Power Station and were removed from the reactor vessel in October 2000. These capsules were received at BWXT Services, Inc. (BWXS) Lynchburg Technology Center (LTC) for testing in late June 2001. The surveillance capsules contained flux wires for neutron flux monitoring, Charpy V-notch impact test specimens fabricated using materials from a variety of sources and thermal monitors [5]. The final evaluation of capsule fluxes and fluences was conducted by TransWare Enterprises Inc. [6].

The results of testing SSP capsules E, F and I are presented in this report. The irradiated material properties are compared to the unirradiated properties to determine the effect of irradiation on material toughness for both base and weld materials, using Charpy V-notch test results. Comparisons have been made with the predictions of Regulatory Guide 1.99, Revision 2 [7].

The information and the associated evaluations provided in this report have been performed in accordance with the requirements of 10CFR50 Appendix B.

Implementation Requirements

The results documented in this report will be utilized by the BWRVIP ISP and by individual utilities to demonstrate compliance with 10CFR50, Appendix H, Reactor Vessel Material Surveillance Program Requirements. Therefore, the implementation requirements of 10CFR50, Appendix H govern and the implementation requirements of Nuclear Energy Institute (NEI) 03-08, Guideline for the Management of Materials Issues, are not applicable.

2
MATERIALS

The chemical compositions, material descriptions and unirradiated (baseline) mechanical properties of the materials irradiated in Oyster Creek Capsules E, F and I are summarized below.

Chemical Compositions

The materials irradiated in Capsules E, F and I are illustrated in Tables 2-1, 2-2 and 2-3. The capsules contained 30 sets of Charpy V-notch specimens representing 21 different materials. Chemical compositions are presented in weight percent. The majority of the materials included in these capsules were archive materials from BWR reactor pressure vessels. Other materials in these capsules are typical of those used in the construction of many operating nuclear reactor pressure vessels. With the exception of CE-1(WM) and CE-2(WM), the materials in Capsules E and I represent different sets of the same materials. The relatively high copper levels in many of these steels are representative of many older reactor vessels.

Table 2-1
Materials Irradiated in SSP (Oyster Creek) Capsule E

Identity	Material	Cu (wt%)	Ni (wt%)	P (wt%)	S (wt%)	Si (wt%)
EP2	Japanese/EPRI Plate (SA533B-1)	**0.06**[2]	**0.59**[2]	**0.006**[2]	**0.008**[2]	**0.22**[2]
A1224-1	Grand Gulf Plate (SA533B-1)	0.03[1] 0.02[1] 0.03[1] Avg. Values	0.67[1] 0.66[1] 0.63[1] **0.65**	0.018[1] 0.011[1] 0.007[1] **0.012**	0.015[1] 0.009[1] **0.012**	0.28[1] 0.28[1] **0.28**
C2331-2	Cooper Plate (SA533B-1)	**0.16**[3]	**0.62**[3]	**0.014**[3]	**0.020**[3]	**0.24**[3]
P2130-2	Nine Mile Point 1 Plate (SA302B, Mod)	**0.172**[3]	**0.584**[3]	**0.018**[3]	**0.028**[3]	**0.17**[3]
C3278-2	FitzPatrick Plate (SA533B-1)	**0.11**[3]	**0.61**[3]	**0.013**[3]	**0.018**[3]	**0.23**[3]
CE-2 (WM)	CE/Linde 1092 #2 Weld (Submerged Arc Weld)	**0.21**[2]	**0.86**[2]	**0.012**[2]	**0.012**[2]	**0.23**[2]
5P6214B	Grand Gulf Weld (Submerged Arc Weld)	0.02[1] 0.00[1] Avg. Values	0.89[1] 0.90[1] **0.90**	0.015[1] 0.009[1] **0.012**	0.017[1] **0.017**	0.43[1] **0.43**
34B009	Millstone 1 Weld (Submerged Arc Weld)	0.16[1] 0.13[1] Avg. Values	1.78[1] 1.84[1] **1.81**	0.017[1] 0.016[1] **0.017**	0.016[1] **0.016**	0.21[1] **0.21**
EP2-21	Quad Cities 2 Weld (Electroslag Weld)	0.12[1] 0.11[1] 0.10[1] Avg. Values	0.25[1] 0.23[1] 0.24[1] **0.24**	0.02[1] 0.015[1] 0.011[1] **0.015**	0.017[1] 0.016[1] **0.017**	0.13[1] 0.13[1] **0.13**
406L44	Quad Cities 1 Weld (Submerged Arc Weld)	0.30[1] 0.29[1] 0.27[1] Avg. Values	0.71[1] 0.68[1] 0.68[1] **0.69**	0.02[1] 0.015[1] 0.012[1] **0.016**	0.018[1] 0.017[1] **0.018**	0.47[1] 0.47[1] **0.47**

1. measured data (from Reference 10).

2. reported values (from Reference 19).

3. best estimate average (from Reference 22).

Table 2-2
Materials Irradiated in SSP (Oyster Creek) Capsule F

Identity	Material	Cu (wt%)	Ni (wt%)	P (wt%)	S (wt%)	Si (wt%)
B&W-1(BM)	B&W/EPRI Plate (SA302B, Mod)	**0.155**[3]	**0.63**[2]	**0.012**[2]	**0.017**[2]	**0.20**[2]
B0673-1	Duane Arnold Plate (SA533B-1)	0.150[4]	0.70[4]	0.006[4]		0.07[4]
		0.150[4]	0.69[4]	0.006[4]		0.06[4]
		0.140[4]	0.62[4]	0.010[4]		0.01[4]
		0.141[4]	0.62[4]	0.014[4]		0.02[4]
		0.141[4]	0.65[4]	0.010[4]		0.09[4]
		0.145[4]	0.61[4]	0.011[4]		0.18[4]
	Avg. Values	**0.15**	**0.65**	**0.010**	N/A	**0.07**
C1079-1	Millstone 1 Plate (SA302B, Mod)	0.2[1]	0.52[1]	0.17[1]	0.028[1]	0.22[1]
		0.23[1]	0.5[1]	0.19[1]		
	Avg. Values	**0.22**	**0.51**	**0.018**	**0.028**	**0.22**
A0610-1	Quad Cities 1 Plate (SA302B, Mod)	0.16[1]	0.53[1]	0.018[1]	0.018[1]	0.17[1]
		0.17[1]	0.54[1]	0.012[1]	0.017[1]	0.2[1]
		0.17[1]	0.50[1]	0.016[1]		
	Avg. Values	**0.17**	**0.52**	**0.015**	**0.018**	**0.19**
A1195-1	HSST-02 Plate (SA533B-1)	0.16[1]	0.71[1]	0.018[1]	0.02[1]	0.22[1]
		0.14[1]	0.68[1]	0.01[1]		
	Avg. Values	**0.15**	**0.70**	**0.014**	**0.020**	**0.22**
B&W-1 (WM)	B&W/EPRI Linde 80 Weld (Submerged Arc Weld)	**0.287**[6]	**0.632**[6]	**0.020**[6]	--[6]	**0.461**[6]
EE/EK	Duane Arnold Weld (Shielded Metal Arc Weld)	0.020[4]	1.00[4]	0.011[4]		0.32[4]
		0.020[4]	0.90[4]	0.010[4]		0.33[4]
		0.025[4]	0.96[4]	0.011[4]		0.02[4]
		0.025[4]	0.94[4]	0.008[4]		0.02[4]
		0.024[4]	0.88[4]	0.010[4]		0.02[4]
	Avg. Values	**0.02**	**0.94**	**0.010**	N/A	**0.14**
FP2-BW	B&W Linde 80 Weld (Submerged Arc Weld)	0.26[1]	0.55[1]	0.018[1]	0.011[1]	0.53[1]
		0.25[1]	0.57[1]	0.01[1]		
	Avg. Values	**0.26**	**0.56**	**0.014**	**0.011**	**0.53**
FP2-6	Humboldt Bay 3 Weld (Submerged Arc Weld)	0.28[1]	0.05[1]	0.017[1]	0.016[1]	0.28[1]
		0.26[1]	0.06[1]	0.015[1]		
	Avg. Values	**0.27**	**0.06**	**0.016**	**0.016**	**0.28**
5P6756	River Bend Weld (Submerged Arc Weld)	**0.06**[5]	**0.93**[5]	**0.009**[5]	**0.015**[5]	**0.40**[5]

1. measured data (from Reference 10).

2. reported values (from Reference 19).

3. estimated values (from Reference 20).

4. measured data from Duane Arnold surveillance capsule report (Reference 21).

5. best estimate average (from Reference 22).

6. average of measured data (from Reference 24).

Table 2-3
Materials Irradiated in SSP (Oyster Creek) Capsule I

Identity	Material	Cu (wt%)	Ni (wt%)	P (wt%)	S (wt%)	Si (wt%)
EP2	Japanese/EPRI Plate (SA533B-1)	**0.06**[2]	**0.59**[2]	**0.006**[2]	**0.008**[2]	**0.22**[2]
A1224-1	Grand Gulf Plate (SA533B-1)	0.03[1] 0.02[1] 0.03[1]	0.67[1] 0.66[1] 0.63[1]	0.018[1] 0.011[1] 0.007[1]	0.015[1] 0.009[1]	0.28[1] 0.28[1]
	Avg. Values	**0.03**	**0.65**	**0.012**	**0.012**	**0.28**
C2331-2	Cooper Plate (SA533B-1)	**0.16**[3]	**0.62**[3]	**0.014**[3]	**0.020**[3]	**0.24**[3]
P2130-2	Nine Mile Point 1 Plate (SA302B, Mod)	**0.172**[3]	**0.584**[3]	**0.018**[3]	**0.028**[3]	**0.17**[3]
C3278-2	FitzPatrick Plate (SA533B-1)	**0.11**[3]	**0.61**[3]	**0.013**[3]	**0.018**[3]	**0.23**[3]
CE-1 (WM)	CE/Linde 1092 #1 Weld (Submerged Arc Weld)	**0.22**[2]	**1.00**[2]	**0.014**[2]	**0.009**[2]	**0.21**[2]
5P6214B	Grand Gulf Weld (Submerged Arc Weld)	0.02[1] 0.00[1]	0.89[1] 0.90[1]	0.015[1] 0.009[1]	0.017[1]	0.43[1]
	Avg. Values	**0.01**	**0.90**	**0.012**	**0.017**	**0.43**
34B009	Millstone 1 Weld (Submerged Arc Weld)	0.16[1] 0.13[1]	1.78[1] 1.84[1]	0.017[1] 0.016[1]	0.016[1]	0.21[1]
	Avg. Values	**0.15**	**1.81**	**0.017**	**0.016**	**0.21**
IP2-21	Quad Cities 2 Weld (Electroslag Weld)	0.12[1] 0.11[1] 0.10[1]	0.25[1] 0.23[1] 0.24[1]	0.02[1] 0.015[1] 0.011[1]	0.017[1] 0.016[1]	0.13[1] 0.13[1]
	Avg. Values	**0.11**	**0.24**	**0.015**	**0.017**	**0.13**
406L44	Quad Cities 1 Weld (Submerged Arc Weld)	0.30[1] 0.29[1] 0.27[1]	0.71[1] 0.68[1] 0.68[1]	0.02[1] 0.015[1] 0.012[1]	0.018[1] 0.017[1]	0.47[1] 0.47[1]
	Avg. Values	**0.29**	**0.69**	**0.016**	**0.018**	**0.47**

1 measured data (from Reference 10).

2 reported values (from Reference 19).

3. best estimate average (from Reference 22).

Material Description

Tables 2-4 and 2-5 contain information about the specimens in SSP (Oyster Creek) Capsules E, F and I including fabricator and copper and nickel content. Table 2-4 presents plate materials and Table 2-5 presents weld materials.

Table 2-4
Plate Materials Irradiated in SSP (Oyster Creek) Capsules E, F and I

Identity (Capsule)	Material Source	Material Type	Cu	Ni	Source (RPV Fabricator)
A1224-1 (E&I)	Grand Gulf	SA533B-1	0.03	0.65	GE (CBIN)
EP2 (E&I)	Japanese/EPRI	SA533B-1	0.06	0.59	CRIEPI
C3278-2 (E&I)	FitzPatrick	SA533B-1	0.11	0.61	GE (CE)
B0673-1 (F)	Duane Arnold	SA533B-1	0.15	0.65	GE (CBIN)
C2331-2 (E&I)	Cooper	SA533B-1	0.16	0.62	GE (CE)
A1195-1 (F)	HSST-02	SA533B-1	0.15	0.70	ORNL (Lukens Steel)
B&W-1(BM) (F)	B&W/EPRI	SA302B, Mod	0.155	0.63	EPRI (B&W)
P2130-2 (E&I)	Nine Mile Point 1	SA302B, Mod	0.172	0.584	GE (CE)
A0610-1 (F)	Quad Cities 1	SA302B, Mod	0.17	0.52	GE (B&W)
C1079-1 (F)	Millstone 1	SA302B, Mod	0.22	0.51	GE (CE)

Table 2-5
Weld Materials Irradiated in SSP (Oyster Creek) Capsules E, F and I

Identity (Capsule)	Material Source	Weld Type	Cu	Ni	Source (RPV Fabricator)
5P6214B (E&I)	Grand Gulf	Submerged Arc Weld	0.01	0.90	GE (CBIN)
EE/EK (F)	Duane Arnold	Shielded Metal Arc Weld	0.02	0.94	GE (CBIN)
5P6756 (F)	River Bend	Submerged Arc Weld	0.06	0.93	GE (CBIN)
EP2-21 & IP2-21 (E&I)	Quad Cities 2	Electroslag Weld	0.11	0.24	GE (B&W)
34B009 (E&I)	Millstone 1	Submerged Arc Weld	0.15	1.81	GE (CE)
CE-2(WM) (E)	CE/EPRI	Submerged Arc Weld, Linde 1092 Flux	0.21	0.86	EPRI (CE)
CE-1(WM) (I)	CE/EPRI	Submerged Arc Weld, Linde 1092 Flux	0.22	1.00	EPRI (CE)
FP2-BW (F)	B&W	Submerged Arc Weld, Linde 80	0.26	0.56	B&W
FP2-6 (F)	Humboldt Bay 3	Submerged Arc Weld	0.27	0.06	GE (CE)
406L44 (E&I)	Quad Cities 1	Submerged Arc Weld	0.29	0.69	GE (B&W)
B&W-1 (WM) (F)	B&W/EPRI Linde 80	Submerged Arc Weld	0.287	0.632	B&W

Unirradiated Properties

CVN Baseline Properties

Tables 2-6, 2-7 and 2-8 provide a summary of the baseline (unirradiated) Charpy V-notch properties of the SSP (Oyster Creek) Capsules E, F and I materials, respectively. In these tables and throughout this report, T_{30} is the 30 ft-lb (40.7 J) transition temperature; T_{50} is the 50 ft-lb (67.8 J) transition temperature; T_{35mil} is the 35 mil (0.89 mm) lateral expansion temperature; and USE is the average energy absorption at full shear. The values provided in these tables were obtained from CVGRAPH [8] hyperbolic tangent curve fits provided in Appendix B. All plate specimens were transverse orientation with the exception of B0673-1 (Duane Arnold plate material), which was longitudinal.

Table 2-6
Baseline CVN Properties of SSP (Oyster Creek) Capsule E

Material Identity	Material	T_{30} °F (°C)	T_{50} °F (°C)	T_{35mil} °F (°C)	Upper Shelf Energy (USE) Ft-lb (J)
EP2	Japanese/EPRI Plate (SA533B-1)	-41.6 (-40.9)	0.7 (-17.4)	-17.9 (-27.7)	109.5 (148.5)
A1224-1	Grand Gulf Plate (SA533B-1)	-20.9 (-29.4)	5.9 (-14.5)	10.9 (-11.7)	147.3 (199.7)
C2331-2	Cooper Plate (SA533B-1)	-13.3 (-25.2)	30.1 (-1.1)	34.1 (1.2)	100.0 (135.6)
P2130-2	Nine Mile Point 1 Plate (SA302B, Mod)	-2.8 (-19.3)	41.6 (5.3)	22.8 (-5.1)	68.2 (92.5)
C3278-2	FitzPatrick Plate (SA533B-1)	-34.4 (-36.9)	5.4 (-14.8)	15.1 (-9.4)	113.3 (153.6)
CE-2(WM)	CE/EPRI Linde 1092 #2 (Submerged Arc Weld)	-96.1 (-71.2)	-45.7 (-43.2)	-62.9 (-52.7)	119.3 (161.7)
5P6214B	Grand Gulf Weld (Submerged Arc Weld)	-26.8 (-32.7)	7.0 (-13.9)	9.2 (-12.7)	91.5 (124.1)
34B009	Millstone 1 Weld (Submerged Arc Weld)	-65.0 (-53.9)	-29.5 (-34.2)	-21.0 (-29.4)	104.4 (141.5)
EP2-21	Quad Cities 2 Weld (Electroslag Weld)	-23.1 (-30.6)	17.9 (-7.8)	22.4 (-5.3)	104.0 (141.0)
406L44	Quad Cities 1 Weld (Submerged Arc Weld)	-8.8 (-22.7)	51.1 (10.6)	39.2 (4.0)	73.3 (99.4)

Table 2-7
Baseline CVN Properties of SSP (Oyster Creek) Capsule F

Material Identity	Material	T_{30} °F (°C)	T_{50} °F (°C)	T_{35mil} °F (°C)	Upper Shelf Energy (USE) Ft-lb (J)
B&W-1(BM)	B&W/EPRI Plate (SA302B, Mod)	-0.7 (-18.2)	40.4 (4.7)	32.9 (0.5)	124.8 (169.2)
B0673-1	Duane Arnold Plate (SA533B-1)	-35.5 (-37.5)	-7.3 (-21.8)	-23.6 (-30.9)	158.1 (214.4)
C1079-1	Millstone 1 Plate (SA302B, Mod)	9.7 (-12.4)	76.6 (24.8)	57.1 (13.9)	61.2 (83.0)
A0610-1	Quad Cities 1 Plate (SA302B, Mod)	-33.5 (-36.4)	-4.1 (-20.1)	-1.5 (-18.6)	101.2 (137.2)
A1195-1	HSST-02 Plate (SA533B-1)	39.8 (4.3)	78.7 (25.9)	79.6 (26.4)	99.7 (135.2)
B&W-1 (WM)	B&W/EPRI Linde 80 (Submerged Arc Weld)	9.6 (-12.4)	69.0 (20.6)	30.8 (-0.7)	80.3 (108.9)
EE/EK	Duane Arnold Weld (Shielded Metal Arc Weld)	-45.4 (-43.0)	-10.2 (-23.4)	-37.3 (-38.5)	99.0 (134.2)
FP2-BW	B&W Linde 80 Weld (Submerged Arc Weld)	40.0 (4.4)	94.9 (34.9)	80.9 (27.2)	75.8 (102.8)
FP2-6	Humboldt Bay 3 Weld (Submerged Arc Weld)	-74.0 (-58.9)	-29.3 (-34.1)	-24.6 (-31.4)	110.3 (149.5)
5P6756	River Bend Weld (Submerged Arc Weld)	-67.1 (-55.1)	-21.3 (-29.6)	-20.3 (-29.1)	104.4 (141.5)

Table 2-8
Baseline CVN Properties of SSP (Oyster Creek) Capsule I

Material Identity	Material	T_{30} °F (°C)	T_{50} °F (°C)	T_{35mil} °F (°C)	Upper Shelf Energy (USE) Ft-lb (J)
EP2	Japanese/EPRI Plate (SA533B-1)	-41.6 (-40.9)	0.7 (-17.4)	-17.9 (-27.7)	109.5 (148.5)
A1224-1	Grand Gulf Plate (SA533B-1)	-20.9 (-29.4)	5.9 (-14.5)	10.9 (-11.7)	147.3 (199.7)
C2331-2	Cooper Plate (SA533B-1)	-13.3 (-25.2)	30.1 (-1.1)	34.1 (1.2)	100.0 (135.6)
P2130-2	Nine Mile Point 1 Plate (SA302B, Mod)	-2.8 (-19.3)	41.6 (5.3)	22.8 (-5.1)	68.2 (92.5)
C3278-2	FitzPatrick Plate (SA533B-1)	-34.4 (-36.9)	5.4 (-14.8)	15.1 (-9.4)	113.3 (153.6)
CE-1(WM)	CE/EPRI Linde 1092 #1 Weld (Submerged Arc Weld)	-41.0 (-40.6)	-5.9 (-21.1)	-39.7 (-39.8)	104.3 (141.4)
5P6214B	Grand Gulf Weld (Submerged Arc Weld)	-26.8 (-32.7)	7.0 (-13.9)	9.2 (-12.7)	91.5 (124.1)
34B009	Millstone 1 Weld (Submerged Arc Weld)	-65.0 (-53.9)	-29.5 (-34.2)	-21.0 (-29.4)	104.4 (141.5)
IP2-21	Quad Cities 2 Weld (Electroslag Weld)	-23.1 (-30.6)	17.9 (-7.8)	22.4 (-5.3)	104.0 (141.0)
406L44	Quad Cities 1 Weld (Submerged Arc Weld)	-8.8 (-22.7)	51.1 (10.6)	39.2 (4.0)	73.3 (99.4)

3
TEST SPECIMEN DESCRIPTION

An inventory of the Charpy specimens contained in SSP (Oyster Creek) Capsules E, F and I is provided in Table 3-1.

Table 3-1
Quantities of Specimens in SSP (Oyster Creek) Capsules E, F and I

Identity: Specimen Code	Capsule	Material	Charpy Specimen Quantity
EP2: EP2-43..84[1]	E	Japanese/EPRI Plate (SA533B-1)	10
A1224-1: EP1-67	E	Grand Gulf Plate (SA533B-1)	10
C2331-2: EP1-30	E	Cooper Plate (SA533B-1)	10
P2130-2: EP1-11	E	Nine Mile Point 1 Plate (SA302B, Mod)	10
C3278-2: EP1-28	E	FitzPatrick Plate (SA533B-1)	10
CE-2 (WM): C211..231[2]	E	CE/EPRI Linde 1092 #2 (Submerged Arc Weld)	10
5P6214B: EP2-67	E	Grand Gulf Weld (Submerged Arc Weld)	10
34B009: EP2-15	E	Millstone 1 Weld (Submerged Arc Weld)	10
DP2-21: EP2-21[3]	E	Quad Cities 2 Weld (Electroslag Weld)	10
406L44: EP2-20	E	Quad Cities 1 Weld (Submerged Arc Weld)	10
EP2: EP2-51..86[4]	I	Japanese/EPRI Plate (SA533B-1)	10
A1224-1: IP1-67	I	Grand Gulf Plate (SA533B-1)	10
C2331-2: IP1-30	I	Cooper Plate (SA533B-1)	10
P2130-2: IP1-11	I	Nine Mile Point 1 Plate (SA302B, Mod)	10
C3278-2: IP1-28	I	FitzPatrick Plate (SA533B-1)	10
CE-1 (WM): C112..132[5]	I	CE/EPRI Linde 1092 #1 (Submerged Arc Weld)	10

Table 3-1
Quantities of Specimens in SSP (Oyster Creek) Capsules E, F and I (Continued)

Identity: Specimen Code	Capsule	Material	Charpy Specimen Quantity
5P6214B: IP2-67	I	Grand Gulf Weld (Submerged Arc Weld)	10
34B009: IP2-15	I	Millstone 1 Weld (Submerged Arc Weld)	10
IP2-21: IP2-21[3]	I	Quad Cities 2 Weld (Electroslag Weld)	10
406L44: IP2-20	I	Quad Cities 1 Weld (Submerged Arc Weld)	10
B&W-1(BM): B01..10[6]	F	B&W/EPRI Plate (SA302B, Mod)	10
B0673-1: ECE..ED2[7]	F	Duane Arnold Plate (SA533B-1)	10
C1079-1: FP1-15	F	Millstone 1 Plate (SA302B, Mod)	10
A0610-1: FP1-20	F	Quad Cities 1 Plate (SA302B, Mod)	10
A1195-1: FP1-H2	F	HSST-02 Plate (SA533B-1)	10
B&W-1(WM): M01..M11[8]	F	B&W/EPRI Linde 80 (Submerged Arc Weld)	10
EE/EK: EEC..EK1[3,9]	F	Duane Arnold Weld (Shielded Metal Arc Weld)	10
FP2-BW: FP2-BW[3]	F	B&W Linde 80 Weld (Submerged Arc Weld)	10
FP2-6: FP2-6[3]	F	Humboldt Bay 3 Weld (Submerged Arc Weld)	10
5P6756: FP2-72	F	River Bend Weld (Submerged Arc Weld)	10

Notes:
1. Charpy specimen codes: EP2-43, -44, -47, -48, -58, -69, -70, -73, -74, -84.
2. Charpy specimen codes: C211, C213, C215, C217, C219, C222, C224, C226, C228, C231.
3. The heat number of these materials is unknown. The specimen code has been used as the specimen identity for clarity.
4. Charpy specimen codes: EP2-51, -52, -55, -56, -60, -77, -78, -81, -82, -86.
5. Charpy specimen codes: C112, C114, C116, C118, C121, C123, C125, C127, C129, C132.
6. Charpy specimen codes: B01, B02, B03, B04, B05, B06, B07, B08, B09, B10.
7. Charpy specimen codes: ECE, ECJ, ECU, ECY, EDB, EDD, EDJ, EDM, EDP, ED2.
8. Charpy specimen codes: M01, M02, M03, M04, M05, M06, M07, M08, M09, M11.
9. Charpy specimen codes: EEC, EEJ, EKA, EKB, EKC, EKE, EKJ, EKT, EKY, EK1.

Charpy V-Notch Specimens

Reference [10] provided the following description of the CVN specimens. The Charpy specimens were full-size Charpy V-notch specimens machined to dimensions as specified in ASTM Specification E185-82 [3]. Plate specimens were removed from both the 1/4T and 3/4T positions and were machined in the transverse direction, with several exceptions discussed below. Weld specimens were removed from all thicknesses of the welded plate except for the surface 0.5 inch (1.3 cm) and the weld root, with several exceptions discussed below. Specimens were machined perpendicular to the length of the weld, with the notch perpendicular to the surface, as specified in ASTM Specification E185-82.

The Duane Arnold plate specimens are archive specimens fabricated at the same time as the standard surveillance specimens. The Duane Arnold plate specimens are longitudinal from the 1/4T or 3/4T thickness with the notch machined perpendicular to the plate surface [10].

The B&W Linde 80 weld (FP2-BW) material was provided in a block with no weld root. The outer surface was removed and discarded. The specimens were fabricated from the remaining material to dimensions as specified in ASTM Specification E185-82.

The EPRI materials [EP2, CE-1(WM), CE-2(WM), B&W-1(BM) and B&W-1(WM)] were provided as finished specimens from several sources.

Dosimeters

Since numerous sets of specimens were placed in each capsule and the capsules are up to 20 inches in vertical height, full length copper and iron flux wires were included. One 1.5-inch long section of iron wire and one 3-inch long section of copper wire, with their center coincident with the center of the Charpy specimen set, were removed from various locations from each of the full capsule length wires. Therefore, a total of ten iron and ten copper wires were prepared for each capsule with one set of iron and copper wires covering a Charpy specimen data set. The numbering system started from top to bottom and left to right. For example, Capsule E#1 iron and copper wires were for Charpy specimen set EP2 43-84 and Capsule E#10 iron and copper wires were for Charpy specimen set EP2-20.

Capsules E and I each had an additional cylinder of special dosimetry. Table 3-2 presents an inventory of the special dosimetry.

Radiometric analysis of the dosimetry is discussed in Section 4 and details of the activity measurements are presented in Appendix D.

Table 3-2
Additional Special Dosimetry in SSP (Oyster Creek) Capsules E, F and I

Content Deleted -
EPRI Proprietary Information

Thermal Monitors

The temperature monitors are quartz tubes containing small cylinders or wires of eutectic material designed to melt within 4°F (2°C) of a specified temperature. The BWR annulus between the vessel wall and the core shroud in the region of the surveillance capsules contains a mix of water returning from the core and feedwater. Depending on feedwater temperature, this annulus region is between 525°F (274°C) and 535°F (279°C). Therefore, temperature monitors designed to melt at specific temperatures provided in Table 3-3 were included in SSP (Oyster Creek) Capsule I.

A visual inspection of each temperature monitor was performed to determine if there was any irregular bending or slumping. These indications were taken as evidence of melting. The results are shown in Table 3-3.

Table 3-3
Thermal Monitors Contained in SSP (Oyster Creek) Capsule I

Content Deleted -
EPRI Proprietary Information

4
MATERIAL IRRADIATION

This chapter describes the irradiation facility, specimen loading within the capsules, radiometric analysis of the dosimetry and fluence evaluation results.

Reactor System Geometry and SSP Surveillance Capsules

The Oyster Creek Nuclear Power Station is a General Electric Company designed BWR/2 located in Forked River, New Jersey. The reactor core consists of 560 fuel assemblies with a rated thermal power of 1930 MWt. Figure 4-1 shows the Oyster Creek core configuration.

Content Deleted -
EPRI Proprietary Information

Figure 4-1
Oyster Creek Core Configuration

Table 4-1 summarizes the reactor system design data for the Oyster Creek reactor. Figures 4-2 through 4-4 contain descriptions of the SSP surveillance capsules in the Oyster Creek reactor.

Table 4-1
Oyster Creek Reactor System Design Data

Content Deleted -
EPRI Proprietary Information

Content Deleted -
EPRI Proprietary Information

Figure 4-2
Oyster Creek SSP Capsule Holder

Content Deleted -
EPRI Proprietary Information

Figure 4-3
Capsules E and F Description

Content Deleted -
EPRI Proprietary Information

Figure 4-4
Capsule I Description

Reactor System Material Compositions

This section defines the material compositions, in terms of atom number densities, for the key reactor system components.

Core Region Materials

The core region is defined by 24 axial homogeneous material zones for each fuel assembly. Each core material zone consists of fuel (^{235}U and ^{238}U), oxygen, Zircaloy, coolant and bypass water. The material composition of each of these material regions varies due to voiding in the core and due to the different fuel design types that constitute the core loading in each of the cycles.

There are six different fuel assembly designs in the Oyster Creek core over cycles 14-17. These fuel designs have axially varying enrichments, as well as different radial enrichment splits and uranium stack densities. The concentration of ^{235}U, ^{238}U, oxygen, zircaloy, coolant and bypass water in each axial node for each assembly type is computed using the volume fractions for each of the constituent materials in the node. These concentrations are assigned to core regions based upon the axial node location and the fuel design type of the fuel assembly at each bundle location in the core. The number densities for hydrogen and oxygen that compose the coolant and bypass regions of the core are based upon the coolant relative water density. The process computer output files contain the coolant relative water density data for selected operating points (designated as state points) in each operating cycle. Saturated water conditions for the core operating condition are shown in Table 4-2.

Table 4-2
Saturated Water at In-core Operating Conditions

Content Deleted -
EPRI Proprietary Information

Ex-Core Region Materials

Saturated water number densities shown in Table 4-2 are also used for water in the reflector and the downcomer regions of the reactor system. Air, which resides in the reactor cavity regions of the system is assumed to be oxygen at a number density of 4.476×10^{-5} atoms/barn-cm. Tables 4-3, 4-4 and 4-5 show the material composition of the shroud, RPV and concrete biological wall, respectively. The core support region consists of saturated water and SS304 stainless steel. The relative densities of each constituent in the core support region are shown in Table 4-6. Similarly, the top guide region is assumed to be composed of voided water and SS304 stainless with relative densities of each constituent shown in Table 4-7.

Table 4-3
Material Composition of the Shroud

Content Deleted -
EPRI Proprietary Information

Table 4-4
Material Composition of the Reactor Pressure Vessel

Content Deleted -
EPRI Proprietary Information

Table 4-5
Material Composition of the Biological Shield Wall

Content Deleted -
EPRI Proprietary Information

Table 4-6
Material Composition of the Core Support Plate Region

Content Deleted -
EPRI Proprietary Information

Table 4-7
Material Composition of the Top Guide Region

Content Deleted -
EPRI Proprietary Information

Reactor Operating Data

Operating plant data must be incorporated into an evaluation of the neutron fluence in a reactor system to ensure that the neutron transport model accurately reflects the actual operating plant conditions throughout the cycles being evaluated. The primary operating system parameters that affect neutron fluence evaluations for BWR's are the plant power level, core relative power distribution, instantaneous void fraction distribution (or equivalently, instantaneous relative water density) and core exposure distribution. In addition, the core loading patterns for the cycles provide the necessary cycle-dependent fuel region composition information.

Plant Power History

Content Deleted -
EPRI Proprietary Information

Cycle State Point Data

The core distribution data (relative power, relative water density and nodal exposure) are obtained from plant process computer edits that were taken at approximately monthly intervals throughout each of the cycles of operation. These process computer edits are considered to be operating state points that are representative of overall plant operation around the time of the edit.

A total of approximately 20 state points for each cycle were provided. A separate neutron transport analysis is carried out for each of the state points in all cycles. Within the period surrounding the state point, the neutron flux distribution is assumed to be constant while the magnitude of the flux is assumed to vary proportionally to the plant power.

Tables 4-8 through 4-11 describe the state point conditions and the corresponding operating dates over which the state point is assumed to be applicable.

Table 4-8
Cycle 14 Operating State Points

Content Deleted -
EPRI Proprietary Information

Table 4-9
Cycle 15 Operating State Points

Content Deleted -
EPRI Proprietary Information

Table 4-10
Cycle 16 Operating State Points

Content Deleted -
EPRI Proprietary Information

Table 4-11
Cycle 17 Operating State Points

Content Deleted -
EPRI Proprietary Information

Core Loading Pattern

The various fuel designs that are present in the core lead to variations in fuel composition throughout the core. Table 4-12 provides a summary of the various fuel designs that were in the Oyster Creek core during cycles 14 through 17. The cycle core loading patterns were used to obtain detailed fuel assembly compositions in the transport analysis models.

Table 4-12
Summary of Oyster Creek Core Loading Pattern

Content Deleted -
EPRI Proprietary Information

Calculation Methodology

In order to perform an accurate evaluation of the neutron fluence accumulation in surveillance capsules and reactor components it is desirable to obtain the detailed three-dimensional flux distribution throughout the reactor system. Regulatory Guide 1.190 [11] describes two basic methodologies that have historically been used to determine the neutron flux distribution in the reactor system. The methodology that has been applied most frequently in the United States is based upon discrete ordinates particle transport techniques. This approach has the advantage of providing a deterministic flux distribution for all modeled regions in the reactor system utilizing relatively efficient solution techniques. The other methodology, which is based upon Monte Carlo particle transport techniques, frequently requires excessive computation time in order to obtain flux distribution solutions with sufficient statistical accuracy. The more traditional discrete ordinate method was used in this evaluation.

Discrete ordinates-based methodologies that provide for detailed modeling of the reactor system in three-dimensions have not been extensively used due to their large computational demands and their limited flexibility in describing complex geometric shapes. As a result, discrete ordinates evaluations are usually performed by combining flux distribution calculations from lower dimension models in order to simulate the detailed three-dimensional flux distribution.

A common method for performing three-dimensional evaluations using lower dimension solutions is based upon the "single channel synthesis" method. The lower dimension solutions are performed using the popular transport code, DORT [12], which can be used to generate one-dimensional and two-dimensional neutron flux distributions.

Three-Dimensional Flux Synthesis

Since the regions of greatest interest in reactor system fluence evaluations are usually best described using cylindrical geometry (e.g., the shroud and RPV), it is common to use flux solutions from various cylindrical models of the reactor system in the three-dimensional flux synthesis process. In this process, the three-dimensional flux distribution is obtained by synthesis of flux solutions from a two-dimensional planar (Rθ) DORT evaluation, a two-dimensional axi-symmetric (RZ) DORT evaluation, and a one-dimensional radial (R) DORT evaluation. The resulting flux at any three-dimensional location is then determined to be:

$$\phi(R,\theta,Z) = \frac{\phi_{R\theta}(R,\theta) \times \phi_{RZ}(R,Z)}{\phi_R(R)}$$

The synthesis operation is carried out using the DOTSYN [13] module of the LEPRICON [14] code package.

Planar (Rθ) Flux Solution Model

The combination of a fairly symmetrical fuel loading pattern in the Oyster Creek core and the radial symmetry of the ex-core reactor system components allows the reactor system to be modeled in octant symmetry with reflected boundaries on the symmetry planes. The model extends radially from the center of the core to the outer surface of the biological concrete shield around the reactor cavity, at which point a vacuum boundary is assumed. The model used in the DORT Rθ solution is composed of 60 angular (θ) mesh intervals with a variable number of radial mesh intervals in each θ interval, ranging from 143 to 172 radial intervals. The ex-core region of the Rθ model consists of nine separate homogeneous material regions: one each for the reflector, shroud, downcomer, RPV liner, RPV, cavity outside the RPV, mirror insulation, cavity outside the insulation and the biological shield wall. Figure 4-5 illustrates the octant Rθ model used in the DORT evaluation of the Oyster Creek reactor system.

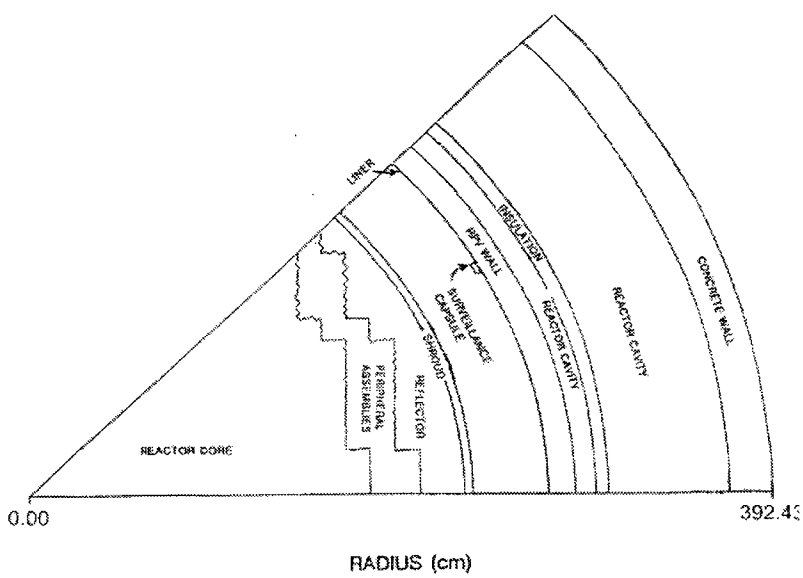

Figure 4-5
DORT Rθ Octant Model of Oyster Creek Reactor

The recommended limitations on mesh size presented in [11] have been followed in laying out the radial and azimuthal meshing in all material regions of the DORT Rθ model.

Since the center of the SSP capsules are located at a core azimuth of 210°, the modeled octant of the core represents the one-eighth reactor azimuthal sector between 180° and 225° (that is, a model azimuth of θ=0° corresponds to a core azimuth of 180° and a model azimuth of θ=45° corresponds to a core azimuth of 225°). Thus the azimuthal center of the surveillance capsules is located at a model azimuth of θ=30°.

Radially, the core region is separated into four homogenized material zones. The zones are composed of fuel assemblies which are selected based upon their distances from an edge face of the core. For example, the outer zone (zone 4) is composed of those assemblies that reside on the core periphery, while zone 3 is composed of those assemblies that are adjacent to a peripheral assembly, etc. Figure 4-6 shows the material zone assignments for the bundles in an octant of the Oyster Creek core. The radial boundaries of the core material zones are computed to preserve the total assembly volume in the material zone.

Content Deleted -
EPRI Proprietary Information

Figure 4-6
Radial Zone Assignement Assemblies in a Core Octant

Anisotropic scattering in the Rθ model is represented with a P_3 Legendre expansion of the scattering cross sections. A symmetric S_8 angular quadrature [15] is used in the DORT solution of the Rθ models.

While it is possible to account for the local flux perturbations resulting from the presence of the SSP capsules by including the capsule geometry in the DORT Rθ model, this approach results in a significant proliferation of individual DORT Rθ models. Many individual DORT Rθ models are generated because all six of the SSP capsules are located at different radii and three of the six capsules were removed after two cycles of operation. In addition, including the surveillance capsule in the Rθ model has the added disadvantage that the synthesized three-dimensional fluxes would include capsule perturbations over the entire height of the reactor system. An alternative approach for dealing with the local perturbations caused by the surveillance capsules that circumvents these disadvantages has been utilized. This alternative approach is described later in this section under "Peripheral Assembly Pin Powers."

A DORT Rθ solution is performed for each state point identified in the section entitled "Cycle State Point Data" in order to account for variations in core power distribution, core void distribution and exposure over the four cycles of operation. For each state point solution, the water densities used in the fuel region of the core are determined from the bundle average water densities for the state point. Similarly, the bundle average powers and exposures are used to obtain the source distribution, using the method described in the section entitled "Neutron Source Generation", for each state point solution. The strong influence of local power resulting from the peripheral bundles is taken into account by including pin-by-pin power distributions for the outer two fuel rows in the Rθ model. The section entitled "Surveillance Capsule Flux Perturbation Calculations" describes the method for determining the relative pin powers for the outer fuel assemblies.

Axi-Symmetric (RZ) Flux Solution Mode

The DORT RZ model is defined axially from the bottom of the core support plate to the top of the top guide. Radially, the DORT RZ model extends from the center of the core to the outer surface of the biological concrete shield. The core centerline is modeled using a reflective boundary, while the top, bottom and outer shield surfaces are modeled using vacuum boundaries.

The core support region of the RZ model extends from the bottom of the core support plate to the bottom of active fuel. The top guide region of the RZ model extends from the top of active fuel to the top of the top guide. The material in each of these regions is homogenized so that the total mass of the components in the region is preserved.

Radially, the core region is separated into four homogenized material zones as described in the section entitled "Planar Flux Solution Model" for the Rθ model. Axially, the core region is modeled using 24 homogeneous material planes, each plane having a height of 15.24 cm. (6.00 inches).

The fuel material in each axial node of each radial zone in the core region is computed using the azimuthally averaged nodal fuel composition for each assembly's fuel design. Water density in each axial node of each radial zone in the core region is similarly computed using azimuthally averaged nodal water densities from the appropriate process computer data file.

The ex-core region of the RZ model consists of nine separate homogeneous material regions: one each for the reflector, shroud, downcomer, RPV liner, RPV, cavity outside the RPV, mirror insulation, cavity outside the insulation and the biological shield wall.

The recommended limitations on mesh size presented in [11] have been followed in laying out the radial and axial meshing in all material regions of the DORT RZ model. The resulting RZ model contains 147 radial intervals and 84 axial intervals. Anisotropic scattering in the RZ model is represented with a P3 Legendre expansion of the scattering cross sections. A symmetric S8 angular quadrature [15] is used in the DORT solution of the RZ models.

A DORT RZ solution is performed for each state point identified in the section entitled "Cycle State Point Data" in order to account for variations in core power distribution, core void distribution and exposure over the four cycles of operation. Each core material zone consists of fuel (^{235}U and ^{238}U), oxygen, Zircaloy-2, coolant and bypass water. For each state point solution, the water densities used in the fuel region of the core are determined from the bundle average water densities for the state point. Similarly, the bundle average powers and exposures are used to obtain the source distribution, using the method described in the section entitled "Neutron Source Generation", for each state point solution.

Radial (R) Flux Solution Model

The DORT R model extends from the center of the core to the outer surface of the biological concrete shield. The material regions in the DORT R model coincide with the RZ model region definitions at a core axial location. Radially, the core region is separated into four homogenized material zones as described in section entitled "Planar Flux Solution Model" for the Rθ model. The nine homogeneous material regions that exist outside the core in the RZ model exist in the R model as well. The radial meshing of the DORT R model coincides with the RZ model and consists of 147 radial intervals.

Anisotropic scattering in the R model is represented with a P3 Legendre expansion of the scattering cross sections. A symmetric S8 angular quadrature [15] is used in the DORT solution of the R models.

A DORT R solution is performed for each state point identified in the section entitled "Cycle State Point Data" in order to account for variations in core power distribution, core void distribution and exposure over the four cycles of operation. Each core material zone consists of fuel (^{235}U and ^{238}U), oxygen, Zircaloy-2, coolant and bypass water. For each state point solution, the water densities used in the fuel region of the core are determined from the bundle average water densities for the state point. Similarly, the bundle average powers and exposures are used to obtain the source distribution, using the method described in the section entitled "Neutron Source Generation", for each state point solution.

Neutron Source Generation

Calculation of the neutron source for the each of the DORT models is performed by the DOTSOR code, a module of the LEPRICON code system. The function of the DOTSOR code is to generate the Rθ source for DORT transport calculations based upon the traditional XY representation of core nodal powers. DOTSOR includes an exposure dependent spectral adjustment for the source contributions from ^{235}U and ^{239}Pu for a single input exposure. The power distributions, provided in the state point process computer data files identified in the section entitled "Cycle State Point Data", are specified in the traditional XY nodal format. Therefore, the nodal power factors, after axial averaging if appropriate, can be used directly in a DOTSOR calculation to obtain the corresponding neutron source distribution for use in a DORT solution.

In order to generate the neutron source for the DORT Rθ model, the relative power input to DOTSOR consists of the axially averaged power factors for each assembly. The exposure for the DORT Rθ source computation is determined as the average of the average peripheral assembly exposures. DOTSOR computes the corresponding neutron source distribution and maps the source terms into the DORT Rθ core mesh regions.

For the DORT RZ model, a separate neutron source distribution is computed for each axial node using the DOTSOR code. For a given axial node, the relative nodal powers, along with the nodal peripheral assembly average exposure is directly input into a DOTSOR computation. The Rθ geometry provided to DOTSOR consists of a single azimuthal sector over the core octant containing the radial mesh from the DORT RZ model. In this fashion, the resulting neutron source is "automatically" averaged in the azimuthal direction by the DOTSOR code. This method also has the advantage that the axial exposure distribution is reflected in the axial neutron source distribution.

The DORT R model neutron source distribution is computed using a combination of the techniques used to compute the DORT Rθ and RZ model source terms. The axially averaged power factors from the DORT Rθ source evaluation are combined with the single azimuthual region Rθ geometry to obtain a power distribution that is averaged both axially and azimuthally.

This technique for generating the neutron source terms for the DORT models results in a total of 26 applications of the DOTSOR code for each state point identified in the section entitled "Cycle State Point Data", i.e. one for the DORT Rθ model, one for the DORT R model and 24 for the DORT RZ model (one for each axial node in the model).

Peripheral Assembly Pin Powers

The strong power gradients present in fuel assemblies located near the edge of the core can have a significant effect on the ex-core neutron flux distribution. Regulatory Guide 1.190 indicates that the pin-by-pin source distributions in peripheral assemblies should be included in best estimate vessel fluence computations.

Pin-by-pin power distributions were not available for Cycles 14 through 17 of the Oyster Creek reactor. As a result, pin-by-pin powers for the outer two rows of fuel assemblies were determined by alternate methods. The assemblies in the outer two core rows can be grouped into four basic groups: (1) peripheral assemblies lying on a side of the core, (2) peripheral assemblies lying in a corner of the core, (3) second row assemblies with a side to the core edge and (4) second row assemblies with a corner on the core edge. Figure 4-7 shows the orientation of these four types of assemblies in the modeled octant of the Oyster Creek reactor.

A DORT Rθ analysis was performed using the k_{eff} solution mode instead of the fixed source mode typical of fluence evaluation solutions. The resulting pin-by-pin fission source terms determined from the DORT solution for the eight by eight pin regions in selected fuel assemblies typical of each peripheral assembly type are then normalized to the average assembly fission source term. The resulting distribution provides an estimate of the relative pin powers for these assemblies. Since there should not be a strong variation in the relative power in edge bundles over the course of a cycle (or even over multiple cycles) the DORT solution was performed using a typical mid-cycle state point (Cycle 15, state point 10).

Content Deleted -
EPRI Proprietary Information

Figure 4-7
Orientation of Peripheral Assembly Types in a Core Octant

Tables 4-13 through 4-16 show the resulting pin by pin relative powers for an eight by eight array for each of the four peripheral assembly types.

Table 4-13
Pin Powers for Eight by Eight Array for Type 1 (Peripheral Side) Assemblies

Content Deleted -
EPRI Proprietary Information

Table 4-14
Pin Powers for Eight by Eight Array for Type 2 (Peripheral Corner) Assemblies

Content Deleted -
EPRI Proprietary Information

Table 4-15
Pin Powers for Eight by Eight Array for Type 3 (2nd Row Side) Assemblies

Content Deleted -
EPRI Proprietary Information

Table 4-16
Pin Powers for Eight by Eight Array for Type 4 (2nd Row Corner) Assemblies

Content Deleted -
EPRI Proprietary Information

Surveillance Capsule Flux Perturbation Calculation

The presence of capsule and pressure vessel sample material inside the surveillance capsules has an effect upon the neutron flux spectrum for regions inside the capsules. It is necessary to correct for these spectral perturbations in order to obtain an accurate prediction of the neutron flux in the capsules. In order to estimate the extent of these spectral perturbations, energy-group dependent flux perturbation factors can be determined. When applied to the unperturbed flux in the surveillance capsule region, these perturbation factors will correctly represent the local effects resulting from the location of each surveillance capsule holder in the surveillance capsules.

There are two different axial locations for the surveillance capsules, one for capsules D, E and F and one for capsules G, H and I. In addition, capsules D, G and H and their containers are only present during cycles 14 and 15. Capsules E, F and I are present throughout cycles 14 through 17.

A series of radial (one-dimensional) DORT calculations were performed to represent the various combinations of capsule locations and cycle variations in capsule content. The calculations are performed in pairs, one in which the actual capsule material is present and one in which the capsule region was represented by water. The ratio of the group-dependent neutron fluxes between each of these paired runs provides a flux multiplication factor that corrects for the surveillance capsule flux perturbations. Tables 4-17 and 4-18 present the flux multiplication factors for cycles 14-15 and 16-17, respectively.

Table 4-17
Capsule Flux Multiplication Factors for Cycles 14 and 15

Content Deleted -
EPRI Proprietary Information

Table 4-18
Capsule Flux Multiplication Factors for Cycles 16 and 17

Content Deleted -
EPRI Proprietary Information

Nuclear Data Library

The nuclear cross section library is an essential element in neutron fluence evaluations. The accuracy of the cross section data is one of the primary factors that governs the accuracy of the neutron fluence prediction in reactor components. Several multi-group cross section libraries have been developed over the years for use in neutron fluence evaluations. The most recent of these libraries is the BUGLE-96 library [16], which has been developed exclusively from ENDF/B-VI nuclear data by Oak Ridge National Laboratory.

Nuclear Cross Sections

BUGLE-96 consists of 47 neutron energy groups that span an energy range of 0.1 eV to 17.332 MeV. The group structure is especially well-suited to applications requiring accurate determination of neutron flux with energy > 1 MeV. This is of primary importance in the evaluation of irradiation damage to reactor components. BUGLE-96 also includes energy group upscattering in the lower (thermal) energy range of < 5.04 eV. This significantly improves the prediction of thermal flux. Table 4-19 shows the group structure for the 47 neutron groups in BUGLE-96. In addition to the neutron cross section set, BUGLE-96 also contains photon fission production and nuclear cross section data to support gamma particle transport calculations. Table 4-20 shows the group structure for the photon cross sections.

The BUGLE-96 library contains an extensive set of nuclide cross sections that are pre-shielded and spectrally collapsed using light water reactor flux spectra. BUGLE-96 incorporates an improved resonance treatment for steel nuclides. The resonance treatment is of particular importance in reactor system component fluence evaluations. Except for oxygen in the reactor cavity regions, the Oyster Creek surveillance capsule evaluations exclusively use pre-shielded and spectrally collapsed cross section data. Table 4-21 lists the nuclides for which pre-shielded and spectrally weighted cross section data is available on BUGLE-96.

BUGLE-96 has been especially developed for the solution of ex-core neutron transport calculations that must account for anisotropic scattering effects. Lighter nuclides contain scattering data for up to P_7 Legendre scattering expansion, while the heavier nuclides contain data for up to P_5 scattering.

Table 4-19
BUGLE-96 Neutron Energy Group Structure (Neutron Cross Section Set)

Content Deleted -
EPRI Proprietary Information

Table 4-20
BUGLE-96 Gamma Energy Group Structure (Photon Cross Section Set)

Content Deleted -
EPRI Proprietary Information

Table 4-21
List of BUGLE 96 Nuclides

Content Deleted -
EPRI Proprietary Information

Table 4-21
List of BUGLE 96 Nuclides (Continued)

Content Deleted -
EPRI Proprietary Information

Table 4-21
List of BUGLE 96 Nuclides (Continued)

Content Deleted -
EPRI Proprietary Information

Table 4-21
List of BUGLE 96 Nuclides (Continued)

Content Deleted -
EPRI Proprietary Information

Activation Response Functions

Response functions are used to calculate nuclear reactions and other integral parameters (e.g., integrated fluxes over various energy ranges) of interest in ex-core calculations. Tables 4-22 and 4-23 list the activation response functions included in the BUGLE-96 nuclear data library.

The response function tables are identified in the BUGLE-96 nuclear data library with the nuclide identifiers 7001, 7002, 7003 and 7004. Response tables 7001 (Part A) and 7002 (Part B) contain response functions which have a flat weighting corresponding to the in-vessel surveillance capsule location. Response tables 7003 (Part A) and 7004 (Part B) contain response functions which have a weighting corresponding to the 1/4 T location in the pressure vessel. These tables include ENDF/B-VI fission spectra (i.e., chi values) for the fissionable nuclides which are used in neutron source calculations.

Table 4-22
Row Positions of Response Functions in BUGLE-96 Tables 7001 and 7003

Content Deleted -
EPRI Proprietary Information

Table 4-23
Row Positions of Response Functions in BUGLE-96 Tables 7002 and 7004

Content Deleted -
EPRI Proprietary Information

Fluence Evaluation Results

This section contains the results from the Oyster Creek fluence analysis. Predicted neutron fluence, neutron flux for energy > 1 MeV and > 0.1 MeV and comparison of the predicted activation to the activation measurements [5] for each capsule are presented. Appendix D contains the details of the procedure and results from the activation measurement. Best estimate neutron fluence and neutron flux for energy > 1 MeV and > 0.1 MeV are also presented for the reactor pressure vessel and reactor shroud at various thicknesses. The measured activity in the E capsule is observed to be consistently lower than the F capsule measurements. One possible explanation for the observation is that the E capsule was positioned behind the F capsule during irradiation. The actual mounting of the capsules has a small impact on the calculated best estimate surveillance capsule flux and fluence since the predicted to measured bias for each capsule is taken into account in determining the best estimate values. Consequently, the results presented in this section assume that the E capsule was inserted in the surveillance capsule holder behind capsule F (as viewed from the core).

Surveillance Capsule Evaluation

Comparison of Predicted Activation to Measurements

Content Deleted -
EPRI Proprietary Information

Table 4-24
Capsule E Iron Flux Wire Comparison

Content Deleted -
EPRI Proprietary Information

Table 4-25
Capsule E Copper Flux Wire Comparison

Content Deleted -
EPRI Proprietary Information

Table 4-26
Capsule E Dosimetry Comparison

Content Deleted -
EPRI Proprietary Information

Table 4-27
Capsule F Iron Flux Wire Comparison

Content Deleted -
EPRI Proprietary Information

Table 4-28
Capsule F Copper Flux Wire Comparison

Content Deleted -
EPRI Proprietary Information

Table 4-29
Capsule I Iron Flux Wire Comparison

Content Deleted -
EPRI Proprietary Information

Table 4-30
Capsule I Copper Flux Wire Comparison

Content Deleted -
EPRI Proprietary Information

Table 4-31
Capsule I Dosimetry Comparison

Content Deleted -
EPRI Proprietary Information

Surveillance Capsule Calculated Neutron Fluence and Flux

Tables 4-32 and 4-33 show the calculated neutron fluence and flux for energy > 1 MeV and > 0.1 MeV, respectively, for capsule E specimen locations. Tables 4-34 and 4-35 show the values for capsule F and Tables 4-36 and 4-37 show the capsule I fluence and flux values for the two energy ranges. These values do not reflect an adjustment for the bias that is observed between predicted and measured activation results.

Table 4-32
Calculated Neutron Fluence and Rated Power Flux for Energy > 1 MeV in Capsule E

Content Deleted -
EPRI Proprietary Information

Table 4-33
Calculated Neutron Fluence and Rated Power Flux for Energy > 0.1 MeV in Capsule E

Content Deleted -
EPRI Proprietary Information

Table 4-34
Calculated Neutron Fluence and Rated Power Flux for Energy > 1 MeV in Capsule F

Content Deleted -
EPRI Proprietary Information

Table 4-35
Calculated Neutron Fluence and Rated Power Flux for Energy > 0.1 MeV in Capsule F

Content Deleted -
EPRI Proprietary Information

Table 4-36
Calculated Neutron Fluence and Rated Power Flux for Energy > 1 MeV in Capsule I

Content Deleted -
EPRI Proprietary Information

Table 4-37
Calculated Neutron Fluence and Rated Power Flux for Energy > 0.1 MeV in Capsule I

Content Deleted -
EPRI Proprietary Information

Surveillance Capsule Best Estimate Neutron Fluence and Flux

Tables 4-38 through 4-43 show the best estimate neutron fluence and flux for energy > 1 MeV and > 0.1 MeV for the three surveillance capsules. The values in these tables have been corrected for the observed bias in the neutron flux based upon comparison to the activation measurements. Flux computation uncertainty (1 standard deviation) resulting from the comparison to activation measurements is shown as well.

Table 4-38
Best Estimate Neutron Fluence and Rated Power Flux for Energy > 1 MeV in Capsule E

Content Deleted -
EPRI Proprietary Information

Table 4-39
Best Estimate Neutron Fluence and Rated Power Flux for Energy > 0.1 MeV in Capsule E

Content Deleted -
EPRI Proprietary Information

Table 4-40
Best Estimate Neutron Fluence and Rated Power Flux for Energy > 1 MeV in Capsule F

Content Deleted -
EPRI Proprietary Information

Table 4-41
Best Estimate Neutron Fluence and Rated Power Flux for Energy > 0.1 MeV in Capsule F

Content Deleted -
EPRI Proprietary Information

Table 4-42
Best Estimate Neutron Fluence and Rated Power Flux for Energy > 1 MeV in Capsule I

Content Deleted -
EPRI Proprietary Information

Table 4-43
Best Estimate Neutron Fluence and Rated Power Flux for Energy > 0.1 MeV in Capsule I

Content Deleted -
EPRI Proprietary Information

5
RESULTS

Charpy V-Notch Testing

Impact Test Procedure

The testing of the Charpy V-notch specimens was performed in accordance with 10CFR50, Appendices G [1] and H [1] and ASTM Specification E185-82 [3].

Charpy impact testing was performed in accordance with Lynchburg Technology Center (LTC) Technical Procedures TP-80 and TP-412, which are in compliance with ASTM E23-94a [17].

For each specimen, impact energy, lateral expansion, percent shear fracture and test temperature were measured and recorded. Impact energy was measured using a Satec S1-1K Impact tester with 240 ft-lb available energy. Lateral expansion was measured using dial indicators mounted on a specialized anvil. Percent shear was estimated by video examination and comparison with the visual standards contained in ASTM E23-94a. The Satec S1-1K impact tester is currently certified by the NIST of Boulder, Colorado; the certification of calibration is available upon request. Test temperature was controlled to ±2°F and monitored using circulating oil heating baths and an ethanol cooling bath with digital temperature controllers. Calibration verification records for temperature measurement are kept on file at BWXS N&EO in accordance with the N&EO Quality Assurance Program.

There are three liquid baths in the FFL for heating/cooling the test specimens.

1. Ethyl Alcohol Bath: -100°F to room temperature
2. Dow Corning 200 fluid (100 cSt. viscosity polydimethylsiloxane): 70°F - 300°F
3. Dow Corning 210 H fluid (100 cSt. viscosity): 150°F - 550°F

Centering tongs for V-notch Charpy specimens of the type shown in ASTM E23-94a were used to center the specimens within the testing machine's anvil.

Lateral expansion and percent shear were measured according to specified methods defined in ASTM E23-98. Percent shear was determined in accordance with Appendix X1 of ASTM E23-98, which involved determining the percent shear value from comparison of the cleavage surface against Figure A6.1. Photographs were taken of both fracture surfaces of the irradiated specimens, which are presented in Appendix C.

Impact Test Results

The results of Charpy V-notch impact tests performed on the various materials contained in the SSP (Oyster Creek) capsules E, F and I are presented in Appendix A, Tables A-1 through A-30. Photographs of the fracture surfaces illustrating the transition in fracture appearance for each irradiated material are provided in Appendix C, Figures C-1 through C-30. The fractures generally show an increasingly ductile or tougher appearance with increasing test temperature.

Analysis of Impact Test Results

A hyperbolic tangent curve-fitting program named CVGRAPH [8] developed by ATI Consulting was used to fit the Charpy V-notch energy data. The impact energy curve-fits from CVGRAPH are provided in Appendix B. Lower shelf energy was fixed at 2.5 ft-lbs (3.4 J) in all cases. Upper shelf energy was fixed at the average of all test energies (at least 3) exhibiting shear greater than or equal to 95%, consistent with ASTM Standard E185-82 [3]. In cases where there were not three data points exhibiting greater than 95% shear, an engineering judgment was made whether the upper shelf should remain free or be fixed at the average of those points with greater than 95% shear.

Irradiated Versus Unirradiated CVN Properties

Tables 5-1, 5-2 and 5-3 summarize the T_{30} [30 ft-lb (40.7 J) Transition Temperature], T_{50} [50 ft-lb (67.8 J) Transition Temperature], T_{35mil} [35 mil (0.89 mm) Lateral Expansion Temperature] and Upper Shelf Energy for the unirradiated and irradiated materials and show the change from baseline values for Capsules E, F and I, respectively. These tables have been sequenced by capsule. The unirradiated and irradiated values are taken from the CVGRAPH tanh fits of Charpy energy data presented in Appendix B. It may be noted that the materials in Capsules E and I [with the exception of CE-1(WM) and CE-2 (WM)] are the same. For ease of comparison of these materials for different flux/fluence, Tables 5-4 through 5-12 present the Capsule E and Capsule I information as provided in Tables 5-1 through 5-3, by material.

Table 5-1
Effect of Irradiation (E>1.0 MeV) on the Notch Toughness Properties of Capsule E Materials

Material Identity[1]	T_{30}, 30 ft-lb (40.7 J) Transition Temperature			T_{35mil}, 35 mil (0.89 mm) Lateral Expansion Temperature			T_{50}, 50 ft-lb (67.8 J) Transition Temperature			CVN Upper Shelf Energy (USE)		
	Unirrad °F (°C)	Irradiated °F (°C)	ΔT_{30} °F (°C)	Unirrad °F (°C)	Irradiated °F (°C)	ΔT_{35mil} °F (°C)	Unirrad °F (°C)	Irradiated °F (°C)	ΔT_{50} °F (°C)	Unirrad ft-lb (J)	Irradiated ft-lb (J)	Change ft-lb (J)
EP2	-41.6 (-40.9)	-18.0 (-27.8)	23.6 (13.1)	-17.9 (-27.7)	15.2 (-9.3)	33.1 (18.4)	0.7 (-17.4)	24.3 (-4.3)	23.6 (13.1)	109.5 (148.5)	94.6 (128.3)	-14.9 (-20.2)
A1224-1	-20.9 (-29.4)	17.2 (-8.2)	38.1 (21.2)	10.9 (-11.7)	49.8 (9.9)	38.9 (21.6)	5.9 (-14.5)	41.2 (5.1)	35.3 (19.6)	147.3 (199.7)	139.8 (189.5)	-7.5 (-10.2)
C2331-2	-13.3 (-25.2)	62.8 (17.1)	76.1 (42.3)	34.1 (1.2)	124.2 (51.2)	90.1 (50.1)	30.1 (-1.1)	105.8 (41.0)	75.7 (42.1)	100.0 (135.6)	82.3 (111.7)	-17.7 (-23.9)
P2130-2	-2.8 (-19.3)	77.1 (25.1)	79.9 (44.4)	22.8 (-5.1)	120.2 (49.0)	97.4 (54.1)	41.6 (5.3)	168.7 (75.9)	127.1 (70.6)	68.2 (92.5)	55.5 (75.2)	-12.7 (-17.2)
C3278-2	-34.4 (-36.9)	23.3 (-4.8)	57.7 (32.1)	15.1 (-9.4)	87.1 (30.6)	72.0 (40.0)	5.4 (-14.8)	67.6 (19.8)	62.2 (34.6)	113.3 (153.6)	95.3 (129.2)	-18.0 (-24.4)

1. Fluence is unique to each specimen set:
   EP2 = 1.6988×10^{18} n/cm^2
   A1224-1 = 1.7116×10^{18} n/cm^2
   C2331-2 = 1.7192×10^{18} n/cm^2
   P2130-2 = 1.7202×10^{18} n/cm^2
   C3278-2 = 1.7135×10^{18} n/cm

Table 5-1
Effect of Irradiation (E>1.0 MeV) on the Notch Toughness Properties of Capsule E Materials (Continued)

Material Identity[1]	T_{30}, 30 ft-lb (40.7 J) Transition Temperature			T_{35mil}, 35 mil (0.89 mm) Lateral Expansion Temperature			T_{50}, 50 ft-lb (67.8 J) Transition Temperature			CVN Upper Shelf Energy (USE)		
	Unirrad °F (°C)	Irradiated °F (°C)	ΔT_{30} °F (°C)	Unirrad °F (°C)	Irradiated °F (°C)	ΔT_{35mil} °F (°C)	Unirrad °F (°C)	Irradiated °F (°C)	ΔT_{50} °F (°C)	Unirrad ft-lb (J)	Irradiated ft-lb (J)	Change ft-lb (J)
CE-2(WM)	-96.1 (-71.2)	96.6 (35.9)	192.7 (107.1)	-62.9 (-52.7)	142.4 (61.3)	205.3 (114.0)	-45.7 (-43.2)	152.7 (67.1)	198.4 (110.3)	119.3 (161.7)	67.7 (91.8)	-51.6 (-70.0)
5P6214B	-26.8 (-32.7)	-22.7 (-30.4)	4.1 (2.3)	9.2 (-12.7)	17.8 (-7.9)	8.6 (4.8)	7.0 (-13.9)	24.0 (-4.4)	17.0 (9.5)	91.5 (124.1)	88.5 (120.0)	-3.0 (-4.1)
34B009	-65.0 (-53.9)	59.5 (15.3)	124.5 (69.2)	-21.0 (-29.4)	97.6 (36.4)	118.6 (65.8)	-29.5 (-34.2)	105.4 (40.8)	134.9 (75.0)	104.4 (141.5)	74.4 (100.9)	-30.0 (-40.7)
EP2-21 (QC2 ESW)	-23.1 (-30.6)	57.5 (14.1)	80.6 (44.8)	22.4 (-5.3)	95.7 (35.4)	73.3 (40.7)	17.9 (-7.8)	94.5 (34.7)	76.6 (42.5)	104.0 (141.0)	94.4 (128.0)	-9.6 (-13.0)
406L44	-8.8 (-22.7)	159.8 (71.0)	168.6 (93.7)	39.2 (4.0)	257.9 (125.5)	218.7 (121.5)	51.1 (10.6)	Note 2	Note 2	73.3 (99.4)	46.8 (63.5)	-26.5 (-35.9)

1. Fluence is unique to each specimen set:
   CE-2(WM) = 1.7572×10^{18} n/cm^2
   5P6214B = 1.7704×10^{18} n/cm^2
   34B009 = 1.7783×10^{18} n/cm^2
   EP2-21 = 1.7794×10^{18} n/cm^2
   406L44 = 1.7724×10^{18} n/cm^2

2. This material did not achieve 50 ft-lbs.

Table 5-2
Effect of Irradiation (E>1.0 MeV) on the Notch Toughness Properties of Capsule F Materials

Material Identity[1]	T_{30}, 30 ft-lb (40.7 J) Transition Temperature			T_{35mil}, 35 mil (0.89 mm) Lateral Expansion Temperature			T_{50}, 50 ft-lb (67.8 J) Transition Temperature			CVN Upper Shelf Energy (USE)		
	Unirrad °F (°C)	Irradiated °F (°C)	ΔT_{30} °F (°C)	Unirrad °F (°C)	Irradiated °F (°C)	ΔT_{35mil} °F (°C)	Unirrad °F (°C)	Irradiated °F (°C)	ΔT_{50} °F (°C)	Unirrad ft-lb (J)	Irradiated ft-lb (J)	Change ft-lb (J)
B&W-1(BM)	-0.7 (-18.2)	43.1 (6.2)	43.8 (24.3)	32.9 (0.5)	80.8 (27.1)	47.9 (26.6)	40.4 (4.7)	86.5 (30.3)	46.1 (25.6)	124.8 (169.2)	94.5 (128.1)	-30.3 (-41.1)
B&W-1(WM)	9.6 (-12.4)	149.8 (65.4)	140.2 (77.8)	30.8 (-0.7)	188.0 (86.7)	157.2 (87.4)	69.0 (20.6)	Note 2	Note 2	80.3 (108.9)	47.3 (64.1)	-33.0 (-44.7)
C1079-1	9.7 (-12.4)	82.8 (28.2)	73.1 (40.6)	57.1 (13.9)	134.6 (57.0)	77.5 (43.1)	76.6 (24.8)	Note 2	Note 2	61.2 (83.0)	49.3 (66.8)	-11.9 (-16.1)
A0610-1	-33.5 (-36.4)	51.7 (10.9)	85.2 (47.3)	-1.5 (-18.6)	97.9 (36.6)	99.4 (55.2)	-4.1 (-20.1)	102.5 (39.2)	106.6 (59.3)	101.2 (137.2)	73.0 (99.0)	-28.2 (-38.2)
A1195-1	39.8 (4.3)	109.1 (42.8)	69.3 (38.5)	79.6 (26.4)	144.0 (62.2)	64.4 (35.8)	78.7 (25.9)	155.9 (68.8)	77.2 (42.9)	99.7 (135.2)	83.2 (112.8)	-16.5 (-22.4)

1. Fluence is unique to each specimen set:
   B&W-1(BM) = 1.8558×10^{18} n/cm^2
   B&W-1(WM) = 1.9189×10^{18} n/cm^2
   C1079-1 = 1.8783×10^{18} n/cm^2
   A0610-1 = 1.8796×10^{18} n/cm^2
   A1195-1 = 1.8725×10^{18} n/cm^2

2. This material did not achieve 50 ft-lbs.

Table 5-2
Effect of Irradiation (E>1.0 MeV) on the Notch Toughness Properties of Capsule F Materials (Continued)

Material Identity	T_{30}, 30 ft-lb (40.7 J) Transition Temperature			T_{35mil}, 35 mil (0.89 mm) Lateral Expansion Temperature			T_{50}, 50 ft-lb (67.8 J) Transition Temperature			CVN Upper Shelf Energy (USE)		
	Unirrad °F (°C)	Irradiated °F (°C)	ΔT_{30} °F (°C)	Unirrad °F (°C)	Irradiated °F (°C)	ΔT_{35mil} °F (°C)	Unirrad °F (°C)	Irradiated °F (°C)	ΔT_{50} °F (°C)	Unirrad ft-lb (J)	Irradiated ft-lb (J)	Change ft-lb (J)
FP2-6 (Humboldt Bay 3 SAW)	-74.0 (-58.9)	29.5 (-1.4)	103.5 (57.5)	-24.6 (-31.4)	87.2 (30.7)	111.8 (62.1)	-29.3 (-34.1)	95.3 (35.2)	124.6 (69.2)	110.3 (149.5)	74.8 (101.4)	-35.5 (-48.1)
5P6756	-67.1 (-55.1)	-5.2 (-20.7)	61.9 (34.4)	-20.3 (-29.1)	31.7 (-0.2)	52.0 (28.9)	-21.3 (-29.6)	39.5 (4.2)	60.8 (33.8)	104.4 (141.5)	79.3 (107.5)	-25.1 (-34.0)
FP2-BW (B&W Linde 80 SAW)	40.0 (4.4)	162.1 (72.3)	122.1 (67.8)	80.9 (27.2)	222.7 (105.9)	141.8 (78.8)	94.9 (34.9)	282.8 (139.3)	187.9 (104.4)	75.8 (102.8)	54.2 (73.5)	-21.6 (-29.3)
B0673-1	-35.5 (-37.5)	37.9 (3.3)	73.4 (40.8)	-23.6 (-30.9)	57.8 (14.3)	81.4 (45.2)	-7.3 (-21.8)	66.9 (19.4)	74.2 (41.2)	158.1 (214.4)	133.0 (180.3)	-25.1 (-34.0)
EE/EK (Duane Arnold SMAW)	-45.4 (-43.0)	-19.1 (-28.4)	26.3 (14.6)	-37.3 (-38.5)	14.2 (-9.9)	51.5 (28.6)	-10.2 (-23.4)	35.5 (1.9)	45.7 (25.4)	99.0 (134.2)	99.0 (134.2)	0 (0)

1. Fluence is unique to each specimen set:
   FP2-6 = 1.9437×10^{18} n/cm^2
   5P6756 = 1.9364×10^{18} n/cm^2
   FP2-BW = 1.9423×10^{18} n/cm^2
   B0673-1 = 1.8699×10^{18} n/cm^2
   EE/EK = 1.9336×10^{18} n/cm^2

Table 5-3
Effect of Irradiation (E>1.0 MeV) on the Notch Toughness Properties of Capsule I Materials

Material Identity[1]	T_{30}, 30 ft-lb (40.7 J) Transition Temperature			T_{35mil}, 35 mil (0.89 mm) Lateral Expansion Temperature			T_{50}, 50 ft-lb (67.8 J) Transition Temperature			CVN Upper Shelf Energy (USE)		
	Unirrad °F (°C)	Irradiated °F (°C)	ΔT_{30} °F (°C)	Unirrad °F (°C)	Irradiated °F (°C)	ΔT_{35mil} °F (°C)	Unirrad °F (°C)	Irradiated °F (°C)	ΔT_{50} °F (°C)	Unirrad ft-lb (J)	Irradiated ft-lb (J)	Change ft-lb (J)
EP2	-41.6 (-40.9)	-16.4 (-26.9)	25.2 (14.0)	-17.9 (-27.7)	19.3 (-7.1)	37.2 (20.7)	0.7 (-17.4)	20.8 (-6.2)	20.1 (11.2)	109.5 (148.5)	97.8 (132.6)	-11.7 (-15.9)
A1224-1	-20.9 (-29.4)	14.2 (-9.9)	35.1 (19.5)	10.9 (-11.7)	56.5 (13.6)	45.6 (25.3)	5.9 (-14.5)	50.5 (10.3)	44.6 (24.8)	147.3 (199.7)	133.8 (181.4)	-13.5 (-18.3)
C2331-2	-13.3 (-25.2)	80.4 (26.9)	93.7 (52.1)	34.1 (1.2)	128.3 (53.5)	94.2 (52.3)	30.1 (-1.1)	128.8 (53.8)	98.7 (54.8)	100.0 (135.6)	80.3 (108.9)	-19.7 (-26.7)
P2130-2	-2.8 (-19.3)	92.2 (33.4)	95.0 (52.8)	22.8 (-5.1)	121.2 (49.6)	98.4 (54.7)	41.6 (5.3)	141.0 (60.6)	99.4 (55.2)	68.2 (92.5)	62.1 (84.2)	-6.1 (-8.3)
C3278-2	-34.4 (-36.9)	34.0 (1.1)	68.4 (38.0)	15.1 (-9.4)	77.6 (25.3)	62.5 (34.7)	5.4 (-14.8)	67.6 (19.8)	62.2 (34.6)	113.3 (153.6)	94.5 (128.1)	-18.8 (-25.5)

1. Fluence is unique to each specimen set:
   EP2 = 2.6016×10^{18} n/cm^2
   A1224-1 = 2.6581×10^{18} n/cm^2
   C2331-2 = 2.7085×10^{18} n/cm^2
   P2130-2 = 2.7548×10^{18} n/cm^2
   C3278-2 = 2.7958×10^{18} n/cm^2

Table 5-3
Effect of Irradiation (E>1.0 MeV) on the Notch Toughness Properties of Capsule I Materials (Continued)

Material Identity[1]	T_{30}, 30 ft-lb (40.7 J) Transition Temperature			T_{35mil}, 35 mil (0.89 mm) Lateral Expansion Temperature			T_{50}, 50 ft-lb (67.8 J) Transition Temperature			CVN Upper Shelf Energy (USE)		
	Unirrad °F (°C)	Irradiated °F (°C)	ΔT_{30} °F (°C)	Unirrad °F (°C)	Irradiated °F (°C)	ΔT_{35mil} °F (°C)	Unirrad °F (°C)	Irradiated °F (°C)	ΔT_{50} °F (°C)	Unirrad ft-lb (J)	Irradiated ft-lb (J)	Change ft-lb (J)
CE-1(WM)	-41.0 (-40.6)	150.9 (66.1)	191.9 (106.6)	-39.7 (-39.8)	191.9 (88.8)	231.6 (128.7)	-5.9 (-21.1)	219.3 (104.1)	225.2 (125.1)	104.3 (141.4)	64.4 (87.3)	-39.9 (-54.1)
5P6214B	-26.8 (-32.7)	-4.3 (-20.2)	22.5 (12.5)	9.2 (-12.7)	42.6 (5.9)	33.4 (18.6)	7.0 (-13.9)	44.9 (7.2)	37.9 (21.1)	91.5 (124.1)	87.7 (118.9)	-3.8 (-5.2)
34B009	-65.0 (-53.9)	74.0 (23.3)	139.0 (77.2)	-21.0 (-29.4)	112.7 (44.8)	133.7 (74.3)	-29.5 (-34.2)	108.4 (42.4)	137.9 (76.6)	104.4 (141.5)	87.0 (118.0)	-17.4 (-23.6)
IP2-21 (QC2 ESW)	-23.1 (-30.6)	53.2 (11.8)	76.3 (42.4)	22.4 (-5.3)	98.4 (36.9)	76.0 (42.2)	17.9 (-7.8)	99.8 (37.7)	81.9 (45.5)	104.0 (141.0)	90.7 (123.0)	-13.3 (-18.0)
406L44	-8.8 (-22.7)	179.9 (82.2)	188.7 (104.8)	39.2 (4.0)	328.3 (164.6)	289.1 (160.6)	51.1 (10.6)	Note 2	Note 2	73.3 (99.4)	42.3 (57.4)	-31.0 (-42.0)

1. Fluence is unique to each specimen set:
   CE-1(WM) = 2.6893×10^{18} n/cm^2
   5P6214B = 2.7478×10^{18} n/cm^2
   34B009 = 2.8000×10^{18} n/cm^2
   IP2-21 = 2.8479×10^{18} n/cm^2
   406L44 = 2.8903×10^{18} n/cm^2

2. This material did not achieve 50 ft-lbs.

Table 5-4
Effect of Irradiation (E>1.0 MeV) on the Notch Toughness Properties of Capsule E and I EP2 Plate Materials[1]

Capsule[2]	T_{30}, 30 ft-lb (40.7 J) Transition Temperature			T_{35mil}, 35 mil (0.89 mm) Lateral Expansion Temperature			T_{50}, 50 ft-lb (67.8 J) Transition Temperature			CVN Upper Shelf Energy (USE)		
	Unirrad °F (°C)	Irradiated °F (°C)	ΔT_{30} °F (°C)	Unirrad °F (°C)	Irradiated °F (°C)	ΔT_{35mil} °F (°C)	Unirrad °F (°C)	Irradiated °F (°C)	ΔT_{50} °F (°C)	Unirrad ft-lb (J)	Irradiated ft-lb (J)	Change ft-lb (J)
E	-41.6	-18.0	23.6	-17.9	15.2	33.1	0.7	24.3	23.6	109.5	94.6	-14.9
	(-40.9)	(-27.8)	(13.1)	(-27.7)	(-9.3)	(18.4)	(-17.4)	(-4.3)	(13.1)	(148.5)	(128.3)	(-20.2)
I	-41.6	-16.4	25.2	-17.9	19.3	37.2	0.7	20.8	20.1	109.5	97.8	-11.7
	(-40.9)	(-26.9)	(14.0)	(-27.7)	(-7.1)	(20.7)	(-17.4)	(-6.2)	(11.2)	(148.5)	(132.6)	(-15.9)

1. These specimens were not tested in a safety related manner.

2. Fluence is unique to each specimen set:
   Capsule E = 1.6988×10^{18} n/cm^2
   Capsule I = 2.6016×10^{18} n/cm^2

Table 5-5
Effect of Irradiation (E>1.0 MeV) on the Notch Toughness Properties of Capsule E and I A1224-1 Grand Gulf Plate Materials

Capsule[1]	T_{30}, 30 ft-lb (40.7 J) Transition Temperature			T_{35mil}, 35 mil (0.89 mm) Lateral Expansion Temperature			T_{50}, 50 ft-lb (67.8 J) Transition Temperature			CVN Upper Shelf Energy (USE)		
	Unirrad °F (°C)	Irradiated °F (°C)	ΔT_{30} °F (°C)	Unirrad °F (°C)	Irradiated °F (°C)	ΔT_{35mil} °F (°C)	Unirrad °F (°C)	Irradiated °F (°C)	ΔT_{50} °F (°C)	Unirrad ft-lb (J)	Irradiated ft-lb (J)	Change ft-lb (J)
E	-13.3	62.8	76.1	34.1	124.2	90.1	30.1	105.8	75.7	100.0	82.3	-17.7
	(-25.2)	(17.1)	(42.3)	(1.2)	(51.2)	(50.1)	(-1.1)	(41.0)	(42.1)	(135.6)	(111.7)	(-23.9)
I	-13.3	80.4	93.7	34.1	128.3	94.2	30.1	128.8	98.7	100.0	80.3	-19.7
	(-25.2)	(26.9)	(52.1)	(1.2)	(53.5)	(52.3)	(-1.1)	(53.8)	(54.8)	(135.6)	(108.9)	(-26.7)

1. Fluence is unique to each specimen set:
   Capsule E = 1.7116×10^{18} n/cm^2
   Capsule I = 2.6581×10^{18} n/cm^2

Table 5-6
Effect of Irradiation (E>1.0 MeV) on the Notch Toughness Properties of Capsule E and I C2331-2 Cooper Plate Materials

Capsule[1]	T_{30}, 30 ft-lb (40.7 J) Transition Temperature			T_{35mil}, 35 mil (0.89 mm) Lateral Expansion Temperature			T_{50}, 50 ft-lb (67.8 J) Transition Temperature			CVN Upper Shelf Energy (USE)		
	Unirrad °F (°C)	Irradiated °F (°C)	ΔT_{30} °F (°C)	Unirrad °F (°C)	Irradiated °F (°C)	ΔT_{35mil} °F (°C)	Unirrad °F (°C)	Irradiated °F (°C)	ΔT_{50} °F (°C)	Unirrad ft-lb (J)	Irradiated ft-lb (J)	Change ft-lb (J)
E	-13.3	62.8	76.1	34.1	124.2	90.1	30.1	105.8	75.7	100.0	82.3	-17.7
	(-25.2)	(17.1)	(42.3)	(1.2)	(51.2)	(50.1)	(-1.1)	(41.0)	(42.1)	(135.6)	(111.7)	(-23.9)
I	-13.3	80.4	93.7	34.1	128.3	94.2	30.1	128.8	98.7	100.0	80.3	-19.7
	(-25.2)	(26.9)	(52.1)	(1.2)	(53.5)	(52.3)	(-1.1)	(53.8)	(54.8)	(135.6)	(108.9)	(-26.7)

1. Fluence is unique to each specimen set:
   Capsule E = 1.7192×10^{18} n/cm^2
   Capsule I = 2.7085×10^{18} n/cm^2

Table 5-7
Effect of Irradiation (E>1.0 MeV) on the Notch Toughness Properties of Capsule E and I P2130-2 Nine Mile Point 1 Plate Materials

Capsule[1]	T_{30}, 30 ft-lb (40.7 J) Transition Temperature			T_{35mil}, 35 mil (0.89 mm) Lateral Expansion Temperature			T_{50}, 50 ft-lb (67.8 J) Transition Temperature			CVN Upper Shelf Energy (USE)		
	Unirrad °F (°C)	Irradiated °F (°C)	ΔT_{30} °F (°C)	Unirrad °F (°C)	Irradiated °F (°C)	ΔT_{35mil} °F (°C)	Unirrad °F (°C)	Irradiated °F (°C)	ΔT_{50} °F (°C)	Unirrad ft-lb (J)	Irradiated ft-lb (J)	Change ft-lb (J)
E	-2.8	77.1	79.9	22.8	120.2	97.4	41.6	168.7	127.1	68.2	55.5	-12.7
	(-19.3)	(25.1)	(44.4)	(-1.5)	(49.0)	(54.1)	(5.3)	(75.9)	(70.6)	(92.5)	(75.2)	(-17.2)
I	-2.8	92.2	95.0	22.8	121.2	98.4	41.6	141.0	99.4	68.2	62.1	-6.1
	(-19.3)	(33.4)	(52.8)	(-5.1)	(49.6)	(54.7)	(5.3)	(60.6)	(55.2)	(92.5)	(84.2)	(-8.3)

1. Fluence is unique to each specimen set:
   Capsule E = 1.7202×10^{18} n/cm^2
   Capsule I = 2.7548×10^{18} n/cm^2

Table 5-8
Effect of Irradiation (E>1.0 MeV) on the Notch Toughness Properties of Capsule E and I C3278-2 FitzPatrick Plate Materials

Capsule[1]	T_{30}, 30 ft-lb (40.7 J) Transition Temperature			T_{35mil}, 35 mil (0.89 mm) Lateral Expansion Temperature			T_{50}, 50 ft-lb (67.8 J) Transition Temperature			CVN Upper Shelf Energy (USE)		
	Unirrad °F (°C)	Irradiated °F (°C)	ΔT_{30} °F (°C)	Unirrad °F (°C)	Irradiated °F (°C)	ΔT_{35mil} °F (°C)	Unirrad °F (°C)	Irradiated °F (°C)	ΔT_{50} °F (°C)	Unirrad ft-lb (J)	Irradiated ft-lb (J)	Change ft-lb (J)
E	-34.4 (-36.9)	23.3 (-4.8)	57.7 (32.1)	15.1 (-9.4)	87.1 (30.6)	72.0 (40.0)	5.4 (-14.8)	67.6 (19.8)	62.2 (34.6)	113.3 (153.6)	95.3 (129.2)	-18.0 (-24.4)
I	-34.4 (-36.9)	34.0 (1.1)	68.4 (38.0)	15.1 (-9.4)	77.6 (25.3)	62.5 (34.7)	5.4 (-14.8)	67.6 (19.8)	62.2 (34.6)	113.3 (153.6)	94.5 (128.1)	-18.8 (-25.5)

1. Fluence is unique to each specimen set:
   Capsule E = 1.7135×10^{18} n/cm^2
   Capsule I = 2.7958×10^{18} n/cm^2

Table 5-9
Effect of Irradiation (E>1.0 MeV) on the Notch Toughness Properties of Capsule E and I 5P6214B Grand Gulf Weld Materials

Capsule[1]	T_{30}, 30 ft-lb (40.7 J) Transition Temperature			T_{35mil}, 35 mil (0.89 mm) Lateral Expansion Temperature			T_{50}, 50 ft-lb (67.8 J) Transition Temperature			CVN Upper Shelf Energy (USE)		
	Unirrad °F (°C)	Irradiated °F (°C)	ΔT_{30} °F (°C)	Unirrad °F (°C)	Irradiated °F (°C)	ΔT_{35mil} °F (°C)	Unirrad °F (°C)	Irradiated °F (°C)	ΔT_{50} °F (°C)	Unirrad ft-lb (J)	Irradiated ft-lb (J)	Change ft-lb (J)
E	-26.8 (-32.7)	-22.7 (-30.4)	4.1 (2.3)	9.2 (-12.7)	17.8 (-7.9)	8.6 (4.8)	7.0 (-13.9)	24.0 (-4.4)	17.0 (9.5)	91.5 (124.1)	88.5 (120.0)	-3.0 (-4.1)
I	-26.8 (-32.7)	-4.3 (-20.2)	22.5 (12.5)	9.2 (-12.7)	42.6 (5.9)	33.4 (18.6)	7.0 (-13.9)	44.9 (7.2)	37.9 (21.1)	91.5 (124.1)	87.7 (118.9)	-3.8 (-5.2)

1. Fluence is unique to each specimen set:
   Capsule E = 1.7704×10^{18} n/cm^2
   Capsule I = 2.7478×10^{18} n/cm^2

Table 5-10
Effect of Irradiation (E>1.0 MeV) on the Notch Toughness Properties of Capsule E and I 34B009 Millstone 1 Weld Materials

Capsule[1]	T_{30}, 30 ft-lb (40.7 J) Transition Temperature			T_{35mil}, 35 mil (0.89 mm) Lateral Expansion Temperature			T_{50}, 50 ft-lb (67.8 J) Transition Temperature			CVN Upper Shelf Energy (USE)		
	Unirrad °F (°C)	Irradiated °F (°C)	ΔT_{30} °F (°C)	Unirrad °F (°C)	Irradiated °F (°C)	ΔT_{35mil} °F (°C)	Unirrad °F (°C)	Irradiated °F (°C)	ΔT_{50} °F (°C)	Unirrad ft-lb (J)	Irradiated ft-lb (J)	Change ft-lb (J)
E	-65.0 (-53.9)	59.5 (15.3)	124.5 (69.2)	-21.0 (-29.4)	97.6 (36.4)	118.6 (65.8)	-29.5 (-34.2)	105.4 (40.8)	134.9 (75.0)	104.4 (141.5)	74.4 (100.9)	-30.0 (-40.7)
I	-65.0 (-53.9)	74.0 (23.3)	139.0 (77.2)	-21.0 (-29.4)	112.7 (44.8)	133.7 (74.3)	-29.5 (-34.2)	108.4 (42.4)	137.9 (76.6)	104.4 (141.5)	87.0 (118.0)	-17.4 (-23.6)

1. Fluence is unique to each specimen set:
   Capsule E = 1.7783×10^{18} n/cm^2
   Capsule I = 2.8000×10^{18} n/cm^2

Table 5-11
Effect of Irradiation (E>1.0 MeV) on the Notch Toughness Properties of Capsule E and I EP2-21 and IP2-21 (QC2 ESW) Weld Materials

Capsule[1]	T_{30}, 30 ft-lb (40.7 J) Transition Temperature			T_{35mil}, 35 mil (0.89 mm) Lateral Expansion Temperature			T_{50}, 50 ft-lb (67.8 J) Transition Temperature			CVN Upper Shelf Energy (USE)		
	Unirrad °F (°C)	Irradiated °F (°C)	ΔT_{30} °F (°C)	Unirrad °F (°C)	Irradiated °F (°C)	ΔT_{35mil} °F (°C)	Unirrad °F (°C)	Irradiated °F (°C)	ΔT_{50} °F (°C)	Unirrad ft-lb (J)	Irradiated ft-lb (J)	Change ft-lb (J)
E	-23.1	57.5	80.6	22.4	95.7	73.3	17.9	94.5	76.6	104.0	94.4	-9.6
	(-30.6)	(14.1)	(44.8)	(-5.3)	(35.4)	(40.7)	(-7.8)	(34.7)	(42.5)	(141.0)	(128.0)	(-13.0)
I	-23.1	53.2	76.3	22.4	98.4	76.0	17.9	99.8	81.9	104.0	90.7	-13.3
	(-30.6)	(11.8)	(42.4)	(-5.3)	(36.9)	(42.2)	(-7.8)	(37.7)	(45.5)	(141.0)	(123.0)	(-18.0)

1. Fluence is unique to each specimen set:
   Capsule E = 1.7794×10^{18} n/cm^2
   Capsule I = 2.8479×10^{18} n/cm^2

Table 5-12
Effect of Irradiation (E>1.0 MeV) on the Notch Toughness Properties of Capsule E and I 406L44 Quad Cities 1 Weld Materials

Capsule[1]	T_{30}, 30 ft-lb (40.7 J) Transition Temperature			T_{35mil}, 35 mil (0.89 mm) Lateral Expansion Temperature			T_{50}, 50 ft-lb (67.8 J) Transition Temperature			CVN Upper Shelf Energy (USE)		
	Unirrad °F (°C)	Irradiated °F (°C)	ΔT_{30} °F (°C)	Unirrad °F (°C)	Irradiated °F (°C)	ΔT_{35mil} °F (°C)	Unirrad °F (°C)	Irradiated °F (°C)	ΔT_{50} °F (°C)	Unirrad ft-lb (J)	Irradiated ft-lb (J)	Change ft-lb (J)
E	-8.8 (-22.7)	159.8 (71.0)	168.6 (93.7)	39.2 (4.0)	257.9 (125.5)	218.7 (121.5)	51.1 (10.6)	Note 2	Note 2	73.3 (99.4)	46.8 (63.5)	-26.5 (-35.9)
I	-8.8 (-22.7)	179.9 (82.2)	188.7 (104.8)	39.2 (4.0)	328.3 (164.6)	289.1 (160.6)	51.1 (10.6)	Note 2	Note 2	73.3 (99.4)	42.3 (57.4)	-31.0 (-42.0)

1. Fluence is unique to each specimen set:
   Capsule E = 1.7724×10^{18} n/cm^2
   Capsule I = 2.8903×10^{18} n/cm^2

2. This material did not achieve 50 ft-lbs.

Discussion

The materials irradiated in SSP (Oyster Creek) Capsules E, F and I exhibited a wide range of radiation embrittlement sensitivity. All but two of the materials experienced less embrittlement than that predicted using U.S. Nuclear Regulatory Commission (USNRC) Regulatory Guide 1.99, Rev. 2 [7] (including margin), based on a unique fluence (E > 1.0 MeV) for each set of specimens. Tables 5-13, 5-14 and 5-15 illustrate this comparison for Capsule E, F and I materials, respectively. Measured shifts that are greater than predicted shifts including margin are shown in bold.

Tables 5-16, 5-17 and 5-18 present a comparison of the predicted upper shelf energy (USE) percent decrease using the USNRC Regulatory Guide 1.99, Rev. 2 figure [7] with the measured percent decrease calculated from the values presented in Tables 5-1 through 5-3. Eighteen out of thirty material data sets exhibited greater than predicted percent decrease in USE. Measured percent decreases that are greater than those predicted are shown in bold.

Table 5-13
Comparison of Actual Versus Predicted Embrittlement of SSP (Oyster Creek) Capsule E Materials

Content Deleted -
EPRI Proprietary Information

Table 5-14
Comparison of Actual Versus Predicted Embrittlement of SSP (Oyster Creek) Capsule F Materials

Content Deleted -
EPRI Proprietary Information

Table 5-15
Comparison of Actual Versus Predicted Embrittlement of SSP (Oyster Creek) Capsule I Materials

Content Deleted -
EPRI Proprietary Information

Table 5-16
Comparison of Actual Versus Predicted Percent Decrease in Upper Shelf Energy (USE) of SSP (Oyster Creek) Capsule E Materials

Content Deleted -
EPRI Proprietary Information

Table 5-17
Comparison of Actual Versus Predicted Percent Decrease in Upper Shelf Energy (USE) of SSP (Oyster Creek) Capsule F Materials

Content Deleted -
EPRI Proprietary Information

Table 5-18
Comparison of Actual Versus Predicted Percent Decrease in Upper Shelf Energy (USE) of SSP (Oyster Creek) Capsule I Materials

Content Deleted -
EPRI Proprietary Information

6
REFERENCES

1. 10 CFR 50, Appendices G (*Fracture Toughness Requirements*) and H (*Reactor Vessel Material Surveillance Program Requirements*), Federal Register, Volume 60, No. 243, dated December 19, 1995.
2. *Fracture Toughness Criteria for Protection Against Failure*, Appendix G to Section III or XI of the ASME Boiler & Pressure Vessel Code, 1995 Edition with addenda through 1996 Addenda.
3. ASTM E185-82, *Standard Practice for Conducting Surveillance Tests for Light-Water Cooled Nuclear Power Reactor Vessels*, E706 (IF), ASTM Standards, Section 3, American Society for Testing and Materials, Philadelphia, PA, 1993.
4. *BWRVIP-87: BWR Vessel and Internals Project Testing and Evaluation of BWR Supplemental Surveillance Program Capsules D, G and H.* EPRI, Palo Alto, CA and BWRVIP: 2000. 1000890.
5. K.Y. Hour, "Evaluation of BWRVIP E, F and I Capsule", BWXT Technologies, Inc., Lynchburg, VA, November 2001.
6. C.H. Potze and K.E. Watkins, "Fluence Calculations for Supplemental Surveillance Capsules E, F and I," TransWare Enterprises Inc., San Jose, Ca, October 2002.
7. USNRC Regulatory Guide 1.99, Revision 2, *Radiation Embrittlement of Reactor Vessel Materials*, United States Nuclear Regulatory Commission, May 1988.
8. CVGRAPH, Hyperbolic Tangent Curve-Fitting Program, Version 5, ATI Consulting, Dublin, CA, March 2002.
9. "Hyperbolic Tangent Curve Fits of Unirradiated Charpy V-notch Impact Test Data for Materials in Capsules E, F and I of the BWR Supplemental Surveillance Program", ATI Consulting, Dublin, CA, June 2001.
10. T.A. Caine, "Progress Report on Phase 2 of the BWR Owners' Group Supplemental Surveillance Program", GE-NE-523-101-1290, GENE, San Jose, CA, January 1992.
11. "Calculation and Dosimetry Methods for Determining Pressure Vessel Neutron Fluence", U. S. Nuclear Regulatory Commission Regulatory Guide 1.190, March 2001.
12. DORT is a module in the DOORS computer code system: "DOORS 3.2: One-, Two- and Three-Dimensional Discrete Ordinates Neutron/Photon Transport Code System", RSICC Computer Code Collection CCC-650, April 1998.
13. "DOTSYN: A module for Synthesizing Three-Dimensional Fluxes in the LEPRICON Computer Code System", RSICC Peripheral Shielding Routine Collection PSR-277, June 1995.

14. "LEPRICON: PWR Pressure Vessel Surveillance Dosimetry Analysis System", RSICC Peripheral Shielding Routine Collection PSR-277, June 1995.

15. J. P. Jenal, P. J. Erickson, W. A. Rhodes, D. B. Simpson and M. L. Williams, "The Generation of a Computer Library for Discrete Ordinates Quadrature Sets", ORNL/TM-6023, September 1977.

16. "Coupled 47 Neutron, 20 Gamma-Ray Group Cross Section Library Derived from ENDF/B-VI for LWR Shielding and Pressure Vessel Dosimetry Applications", RSICC Data Library Collection DLC-185, March 1996.

17. ASTM E23-94a, *Standard Test Methods for Notched Bar Impact Testing of Metallic Materials*, ASTM Standards, Section 3, American Society for Testing and Materials, Philadelphia, PA, 1994.

18. "Hyperbolic Tangent Curve Fits of Charpy V-notch Impact Test Data for Materials Irradiated in Capsules E, F and I of the BWR Supplemental Surveillance Program", ATI Consulting, Dublin, CA, October 2002.

19. "Integrated Reactor Vessel Surveillance Program, A Joint EPRI-CRIEPI RPV Embrittlement Study", Program Update Report, Volume 1, ATI Consulting, December 1995.

20. Letter, W.L. Server (ATI Consulting) to R.G. Carter (EPRI), Reassessment of EPRI-CRIEPI Joint Program Materials Heat Identities and Chemistries, October 25, 2002.

21. L.J. Tilley, "Duane Arnold RPV Surveillance Materials Testing and Analysis," GE-NE-B1100716-01, Revision 0, July 1997.

22. *BWRVIP-135: BWR Vessel and Internals Project, Integrated Surveillance Program (ISP) Data Source Book and Plant Evaluations*. EPRI, Palo Alto, CA: 2004. 1011019.

23. Framatome ANP Engineering Information Record 51-5023275-00, "Charpy Impact Testing of Oconee 1 Plate Material," December 20, 2002.

24. BWX Technologies, Inc., Letter (K. Hour) Letter to EPRI (R. Carter) dated April 16, 2003: Analysis Report #0302009, "ICP Metals Analysis of NME Samples."

A
SUMMARY OF CHARPY V-NOTCH TEST DATA

The following pages provide the irradiated Charpy V-notch test data for each specimen in tabular form. All values have been rounded.

Content Deleted -
EPRI Proprietary Information

B
TANH CURVE FIT PLOTS OF CVN TEST DATA

Ten (10) Charpy V-Notch specimens of each irradiated plate and weld material were tested at temperatures selected to define the toughness transition and upper shelf portions of the fracture toughness curves. The absorbed energy and lateral expansion data were fit with the hyperbolic tangent function of CVGRAPH [8]. The absorbed energy data and fit plots are presented in this Appendix. Unirradiated data for the same materials were also fit and are presented for comparison. The curves have been sequenced by material in order of unirradiated, followed by irradiated.

Content Deleted -
EPRI Proprietary Information

C
CVN FRACTURE APPEARANCE PHOTOGRAPHS

Photographs of each Charpy specimen fracture surface were taken per the requirements of ASTM E185-82 [3].

Content Deleted -
EPRI Proprietary Information

D
DOSIMETER ANALYSIS

All dosimeters were recovered from the capsules and there were no deviations noted. The reactor shut down time was October 13, 2000. All dosimeters were cleaned and prepared. Dosimeters were washed in reagent grade acetone, blotted dry with a laboratory towel, their dimensions measured with a certified micrometer caliper and weighed on a certified analytical balance. Each dosimeter was then mounted in the center of a PetriSlide™ with double-sided tape.

Quantitative Gamma Spectrometry

Selected dosimeters, in the PetriSlide™ (point source), were given a 300 second preliminary count on the 31% PGT gamma spectrometer. This provided information with which to judge the best distance to count the dosimeter to get a minimum of 10,000 counts in the photopeak of interest while keeping the counter dead time below 15%. The spectra were then measured quantitatively at the appropriate counting positions and for the appropriate count times determined from the preliminary counts. The activities of the dosimeters were quantified by the spectral gamma rays listed in the table below:

Table D-1
Table of Quantifying Gamma Rays

Dosimeter	Analyte
Cobalt	^{60}Co @ 1332 keV from ^{59}Co
Iron	^{54}Mn @ 834 keV from ^{54}Fe
Niobium	^{93m}Nb @ 16.6 keV from ^{93}Nb ^{182}Ta @ 1122 keV from Tantalum Impurity ^{94}Nb @ 871 keV from Niobium Activation
Nickel	^{58}Co @ 811 keV from ^{58}Ni
Titanium	^{46}SC @ 1121 keV from ^{46}Ti
Silver	^{110m}Ag @ 658 keV from ^{109}Ag
Copper	^{60}Co @ 1332 keV from ^{63}Cu
^{235}U	^{137}Cs @ 662 keV

Geometry Corrections for Wire and Foil Type Dosimeters

The detector was calibrated for the foil and wire dosimeters with a "point source" standard. A NIST-traceable mixed gamma standard was used. The wires, foils and beads were not identical to the point source, so corrections for the differences between the dosimeter and the standard were required.

The point source standard was made up of a mixed gamma ray source which was sandwiched between two pieces of film. The source was actually a spot a few millimeters in diameter and was very thin. The calibration was performed with this source mounted against the surface of a PetriSlide™, oriented with the plane of the spot parallel to the face of the detector. The dosimeters were mounted on a thin piece of double-sided adhesive tape in the center of the face of a PetriSlide™. This placed the closest point on the dosimeter at the plane of the calibration source, with the bulk of it at some distance from the calibration distance.

The area covered by the dosimeter was not greatly different from that of the standard source spot. A correction was made for the slight difference in distance between the center of mass of the wire or foil and center of mass of the standard point source in the following manner. It was assumed that the activity was distributed uniformly throughout the dosimeter. The dosimeter was partitioned into four slabs parallel to the face of the detector and a weighted average $1/r^2$ correction for the distance between the center of each slab and the plane of the calibration source was calculated. The weight factor was based on the relative mass of each slab. Since it was assumed that the dosimeter was uniform in composition, the weight factors were proportional to the cross-sectional area of each slab.

The weighted correction factor, F_G, was given by:

$$F_G = \sum_{i=1}^{4} W_i \left(\frac{R_0}{R_i} \right)^2$$

where F_G was the weighted correction factor, W_i was the weight factor for each slab, R_0 was the distance from the detector face to the plane of the calibration standard [D-1] and R_i was the distance from the detector face to the center of each slab. The distance R_0 was measured directly for the detector/sample holder combination used. The distance R_i was the sum of this distance and the distance between the plane of the standard and the center of each slab.

Wire Type Dosimeters

For a wire of diameter D, these are:

$$R_1 = R_0 + \frac{D}{8}$$

$$R_2 = R_0 + 3\frac{D}{8}$$

$$R_3 = R_0 + 5\frac{D}{8}$$

$$R_4 = R_0 + 7\frac{D}{8}$$

The weight factors sum to unity. They were derived from the cross-sectional area which is a circle. This circle was divided into four slabs of equal thickness, the thickness of which was D/4=r/2, where r was the radius of the wire.

Two of the slabs were circular segments and the other two were slices of the circle. This is shown schematically in Figure D-1.

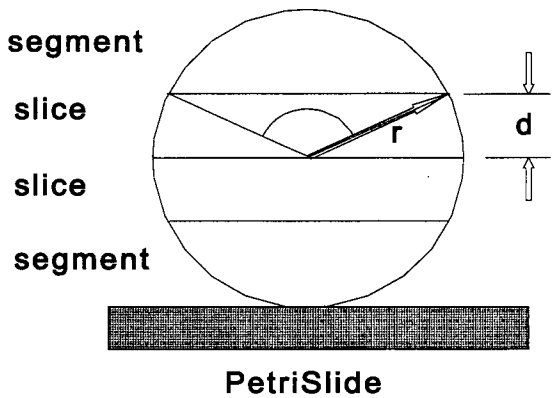

Figure D-1
Wire on PetriSlide™

$$r = radius\ of\ wire$$

$$d = \frac{r}{2}$$

$$\theta = 2\,\mathrm{Cos}^{-1}\left(\frac{d}{r}\right)$$

$$K_{segment} = \left(\frac{1}{2}\right) r^2 (\theta - \mathrm{Sin}(\theta))$$

$$K_{circle} = \pi r^2$$

$$K_{slice} = \left(\frac{1}{2}\right) K_{circle} - K_{segment}$$

$$W_{segment} = \frac{K_{segment}}{K_{circle}} = 0.1955$$

$$W_{slice} = 0.5 - W_{segment} = 0.3045$$

The areas K were calculated for a wire of unit radius. The weight factors for the slabs were calculated as the ratios of the segment or slice to the area of the circle.

Foil Type Dosimeters

For a foil type dosimeter, the same type of equations as the wire dosimeter are used. The R_i distance factors for a foil of thickness T would be:

$$R_1 = R_0 + \frac{T}{8}$$

$$R_2 = R_0 + 3\frac{T}{8}$$

$$R_3 = R_0 + 5\frac{T}{8}$$

$$R_4 = R_0 + 7\frac{T}{8}$$

As before, the weight factors sum to unity. They are derived by dividing a foil of unit thickness into four equal slabs. This is shown schematically in Figure D-2.

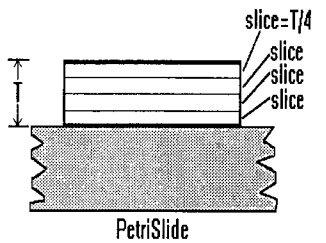

Figure D-2
Foil on PetriSlide™

The measured activities were corrected for the geometry offset by dividing the activities by the weighted correction factor F_G.

Attenuation Corrections for Wire and Foil Type Dosimeters

The self-absorption of low energy gamma rays in some of the dosimeters can be significant, depending on the energy of the gamma-ray photon, the composition and the diameter or thickness of the dosimeter. Self-absorption corrections were calculated for all of the gamma-ray and dosimeter combinations.

Wire Type Dosimeter

The cylindrical wire source model of Evans and Evans [D-2] was used to compute the self-absorption factors for the wires. Equations 26 and 27 of Evans and Evans [D-2] were used for the calculations.

$$N_2 = N_0\left[G_2 - \left(\frac{8}{3\pi}\right)\mu r U_2 + \left(\frac{1}{2}\right)\mu^2 r^2 V_2 - \left(\frac{32}{45\pi}\right)\mu^3 r^3 W_2 + \left(\frac{1}{12}\right)\mu^4 r^4 X_2 + \ldots\right],$$

with :

$$G_2 = 1 + \left(\frac{1}{2}\right)\left(\frac{r^2}{R_0^2}\right) + \left(\frac{5}{8}\right)\left(\frac{r^4}{R_0^4}\right) + \ldots,$$

$$U_2 = 1 - \left(\frac{3\pi}{16}\right)\left(\frac{r}{R_0}\right) + \left(\frac{3}{5}\right)\left(\frac{r^2}{R_0^2}\right) - \left(\frac{5\pi}{32}\right)\left(\frac{r^3}{R_0^3}\right) + \ldots,$$

$$V_2 = 1 - \left(\frac{128}{45\pi}\right)\left(\frac{r}{R_0}\right) + \left(\frac{5}{6}\right)\left(\frac{r^2}{R_0^2}\right) + \ldots,$$

$$W_2 = 1 - \left(\frac{45\pi}{128}\right)\left(\frac{r}{R_0}\right) + \ldots,$$

$$X_2 = 1 - \ldots,$$

and,

N_0 = the true "point source" activity,

N_2 = self-absorption corrected activity,

r = wire radius,

R_0 = wire-to-detector distance, cm,

μ = $\rho\mu_0$ = linear attenuation coefficient cm^{-1},

ρ = density, G/cm^3,

μ_0 = mass attenuation coefficient, cm^2/G.

Foil Type Dosimeter

The linear source model by W.R. Dixon [D-3] was used to calculate the self-absorption for foil dosimeters.

$$\frac{I_0}{I} = \frac{\mu T}{1 - \exp^{-}\mu T}$$

where: $\mu = \rho\mu_0$ = linear attenuation coefficient cm^{-1},

ρ = density, G/cm^3,

μ_0 = mass attenuation coefficient, cm^2/G.

T = average foil thickness, cm.

I = Intensity

I_0 = Initial Intensity

Values for density were taken from the CRC Handbook of Chemistry and Physics, 63rd Edition [D-4]). Values for the mass attenuation coefficients were interpolated from the Storm and Israel tables [D-5]. The log-log polynomial technique of Hsu and Dowdy [D-6] was used for the interpolation.

Dosimeter Specific Activities

The elemental weight fractions of the dosimeters were taken from the EPRI RFQ [D-7]. The isotopic weight fractions of the target nuclides were taken from the CRC tables [D-4]. These are listed in Table D-2.

Table D-2
Isotopic Fractions and Weight Fractions of Target Nuclides

Content Deleted -
EPRI Proprietary Information

The weight fraction of the target nuclide listed in the data tables is the product of the isotopic weight fraction of the target and the elemental weight fraction of the element in the dosimeter.

The niobium dosimeters were analyzed by measuring the ^{93m}Nb activity at 16 KeV on a low energy photon detector (LEPS) using Monte Carlo techniques [D-8] to correct for fluorescence from ^{94}Nb and ^{182}Ta which were measured by gamma spectroscopy.

The uncertainty values stated in the data tables are representative only of uncertainty in measurements taken at Nuclear Environmental Laboratory Services and are not intended to be all-encompassing. Uncertainties in parameters such as density, half-life, gamma yields, branching ratios, etc. are not included in these figures, but certainly do contribute to the overall uncertainty. The systematic uncertainty column that appears in the data tables is the uncertainty that results from the calibration of standardized analytical equipment, except for the niobium dosimeters, where the systematic uncertainty is estimated to be 10% [D-9].

The dosimeter specific activities were calculated by dividing the corrected activity of the analyte nuclide by the target nuclide mass. Note that decay correction was already made in the data and should not be made again.

Table D-3
Specific Activities of BWR VIP Capsules E/F and I Dosimetry

Content Deleted -
EPRI Proprietary Information

Table D-3
Specific Activities of BWR VIP Capsules E/F and I Dosimetry (Continued)

Content Deleted -
EPRI Proprietary Information

Table D-3
Specific Activities of BWR VIP Capsules E/F and I Dosimetry (Continued)

Content Deleted -
EPRI Proprietary Information

References

D-1. J. L. Coor, "Source-to-Detector Information for Various Gamma Detectors - Point Source Geometry", B&W NESI Report File 93:E84923:001 (November 1993).

D-2. R. D. Evans and R. O. Evans, "Studies of Self-Absorption in Gamma-Ray Sources", Reviews of Modern Physics, *20*, pp. 305-326, (January 1948).

D-3. W. R. Dixon, "Self-Absorption Corrections for Large Gamma Ray Sources", NUCLEONICS, Volume 8, Number 4, pg. 69, (April, 1951).

D-4. R. C. Weast and M. J. Astle, Eds., "CRC Handbook of Chemistry and Physics, 63rd Ed.", CRC Press, Boca Raton, FL, 1982.

D-5. E. Storm and H. I. Israel, "Photon Cross Sections from 0.001 to 100 MeV for Elements 1 through 100", Los Alamos Scientific Laboratory of the University of California, Los Alamos, NM, LA-3753, UC-34, PHYSICS, TID-4500, June 1967.

D-6. H. H. Hsu and E. J. Dowdy, "An Interpolation Technique for Gamma-Ray Attenuation Coefficients from 40 keV to 15 MeV", Nuclear Instruments and Methods, *204*, pp. 505-509 (1983).

D-7. EPRI RFP47798-1QA "BWRVIP Integrated Surveillance Program - Testing of Supplemental Surveillance Capsules E, F and I Irradiated in Oyster Creek", April 11, 2000.

D-8. T. G. Williamson and A. C. Chubb, "Niobium Foil, Counting and Correction for Niobium X-rays from Trace Isotopes", Department of Nuclear Engineering and Engineering Physics, University of Virginia, Charlottesville, Virginia, Report No. UVA/532886/NEEP90/102, dated August 1989.

D-9. J. L. Coor, "Uncertainty Assessment and Results of Niobium Analysis for Davis Besse Cavity Dosimetry Benchmark Experiment", B&W NESI Report No. 93:136146:01 (July 1993).

E
RECORD OF REVISIONS

BWRVIP-111, Revision 1	Information from the following documents was used in preparing the changes included in this revision of the report: 1. *BWRVIP-135: BWR Vessel and Internals Project, Integrated Surveillance Program (ISP) Data Source Book and Plant Evaluations*, EPRI, Palo Alto, CA: 2004. 1011019. 2. Framatome ANP, Engineering Information Record 51-5023275-00, "Charpy Impact Testing of Oconee 1 Plate Material," December 20, 2002. 3. GE-NE-523-99-0792, "Progress Report on Phase 2 of the BWR Owners' Group Supplemental Surveillance Program," GE Nuclear Energy, January 1992. 4. BWX Technologies, Inc., Letter (K. Hour) Letter to EPRI (R. Carter) dated April 16, 2003: Analysis Report #0302009, "ICP Metals Analysis of NME Samples." Details of the revisions can be found in Table E-1.

Table E-1
Revision Details

Required Revision	Source of Requirement for Revision	Description of Revision Implementation
SECTION 1, INTRODUCTION	NEI 03-08	Implementation Requirements added.
SECTION 2, MATERIALS		
Update the best estimate chemistry values for plate heats C2331-2, P2130-2, and C3278-2 and weld heat 5P6756 in Tables 2-1 through 2-5.	Reference 1.	The chemistry values originally reported were based on the chemistry measurements made by GE at the time the SSP capsules were assembled [3]. Subsequent to the publication of the original issue of this report, the BWRVIP found additional chemistry measurements for these surveillance materials from the source plant records. Reference 1 calculated a revised best estimate based on all valid data. Tables 2-1 through 2-5 were updated to show the latest best estimate chemistry values for these surveillance materials.
Update the best estimate chemistry for weld heat B&W-1(WM) in Tables 2-2 and 2-5.	Reference 4.	Chemistry testing on broken specimens was conducted in 2003 and reported by Reference 4.
Correct the discussion in *CVN Baseline Properties*, which incorrectly identifies A1195-1 specimens as longitudinal.	Reference 3.	A1195-1 specimens are transverse (TL). The statement that they are LT was deleted.
Update the baseline Charpy properties of plate heat P2130-2 and weld heat 406L44 in Tables 2-6 and 2-8.	Reference 1	These materials are used in the BWRVIP ISP. Subsequent to the original issue of this capsule report, additional analyses of the CVN properties were conducted and documented in Reference 1. Additional, valid baseline data for the material was found for P2130-2 and included in the analysis. The baseline values reported in Tables 2-6 and 2-7 were updated to be consistent with the values used in the BWRVIP ISP *BWRVIP-135 Data Source Book* for ISP implementation. The updated curve fits are provided in Appendix B.

Table E-1
Revision Details (Continued)

Required Revision	Source of Requirement for Revision	Description of Revision Implementation
Correct the baseline Charpy properties of plate heat B&W-1(BM) in Table 2-7.	Reference 2.	The baseline Charpy values originally reported in Table 2-7 for B&W-1(BM) were incorrect; the fabricator had reported the HAZ Charpy data as being the base plate data. Archive material for this heat was retested, and in addition the correct original baseline data were identified. The combined baseline data were fit by CVGRAPH and are reported in Table 2-7. The updated curve fit is provided in Appendix B.
SECTION 3, TEST SPECIMEN DESCRIPTION		
In the second paragraph under *Charpy V-notch Specimens*, delete the first sentence, which states that A1195-1 is LT.	Reference 3.	A1195-1 specimens are TL. The sentence was deleted.
Add discussion of the results of the inspection of the thermal monitors in Capsule I.		A report of the visual inspection of the monitors was added. A column was added to Table 3-3 (Thermal Monitors Contained in SSP Capsule I) to indicate, for each monitor, whether or not it exhibited signs of melting.
SECTION 4, MATERIAL IRRADIATION		No revisions.
SECTION 5, RESULTS		
In the discussion *Irradiated versus Unirradiated CVN Properties*, delete the reference to the specific sources of the CVGRAPHs. Reference to ATI calculation packages is not appropriate or necessary, and the specific packages have been superseded by more recent work.	Editorial.	In the discussion *Irradiated versus Unirradiated CVN Properties*, deleted reference to the specific sources of the CVGRAPHs (References 9 and 18).

Table E-1
Revision Details (Continued)

Required Revision	Source of Requirement for Revision	Description of Revision Implementation
Tables 5-1 and 5-3: Update the baseline notch toughness properties for P2130-2 and weld 406L44 and revise calculated shifts resulting from the updated baseline values.	Reference 1.	The values shown in this table were updated to reflect the values from updated tanh curve fits for these materials. The updated baseline (unirradiated) Charpy energy curve fits are presented in Appendix B.
Table 5-2: Number the table footnotes.	Editorial.	
Table 5-2: Update the baseline notch toughness properties for B&W-1(BM) and revise the calculated shifts resulting from the change.	Reference 4.	The baseline (unirradiated) values shown in this table were updated to reflect the values from updated tanh curve fit for B&W-1(BM), based on new test data. The updated baseline Charpy energy curve fit is presented in Appendix B.
Table 5-7: Update the baseline Charpy values and calculated shifts based on the changes for P2130-2 in Table 5-1 and 5-3.		Table 5-7 is a repeat of the data for P2130-2 in Tables 5-1 and 5-3.
Table 5-12: Update the baseline Charpy values and calculated shifts based on the changes for 406L44 in Table 5-1 and 5-3.		Table 5-12 is a repeat of the data for 406L44 in Tables 5-1 and 5-3.
Update the *Discussion* section to reflect changes in the number of materials experiencing more embrittlement than predicted.by Reg. Guide 1.99 Rev. 2.	Editorial.	Two materials experiences more embrittlement than predicted by Reg. Guide 1.99 Rev. 2, and 18 materials experiences a greater percent decrease in USE than predicted by reg. Guide 1.99 Rev. 2.
Update Tables 5-13, 5-14, and 5-15 which compare the actual versus predicted embrittlement of the capsule specimens.	Best estimate chemistry and baseline Charpy changes discussed above.	As a result of revised best estimate chemistries for C2331-2, P2130-2, C3278-2, and B&W-1(WM), those materials have revised predicted shifts. As a result of the revised baseline (unirradiated) Charpy properties of P2130-2, 406L44 and B&W-1(BM), those materials have revised measured shifts. Minor changes (e.g., 0.1 °F or °C) were also made as required to the predicted shifts of some other materials as a result of more precise, refreshed calculations for all materials.

Table E-1
Revision Details (Continued)

Required Revision	Source of Requirement for Revision	Description of Revision Implementation
Update the Tables 5-16, 5-17, and 5-18 for the updated best estimate Cu and the measured decrease in USE for affected materials.	Reference 1.	P2130-2, 406L44, and B&W-1(BM) materials were updated for % USE decrease resulting from revised baseline CVN curve fits. The predicted % decrease in USE for C2331-2, P2130-2, C3278-2 and 5P6756 were updated for revised best estimate Cu content of those materials; the revised predicted shifts were taken from Reference 1.
SECTION 6, REFERENCES		
Add references as required.	Editorial.	BWRVIP-135 was added as Reference 22. Framatome testing report for B&W-1(BM) was added as Reference 23. BWXT chemistry testing report on B&W-1(WM) was added as Reference 24.
APPENDIX A, SUMMARY OF CHARPY V-NOTCH TEST DATA		No revisions.
APPENDIX B, TANH CURVE FIT PLOTS OF CVN TEST DATA		
Replace Figures B-10 with updated baseline curve fit for heat P2130-2.	Reference 1.	Additional baseline data was included in a revised fit as reported in Reference 1.
Replace Figure B-29 with updated baseline curve fit for heat 406L44.	Reference 1.	The fixed USE for this fit was recalculated for improvement in the quality of the tanh fit as provided in Reference 1.
Replace Figure B-32 with updated baseline curve fit for heat B&W-1(BM).	Reference 2.	The baseline data originally reported for B&W-1(BM) was incorrect. Additional baseline Charpy testing was conducted by Reference 2. ATI fit the data to a tanh curve and the updated curve fit is provided.

Table E-1
Revision Details (Continued)

Required Revision	Source of Requirement for Revision	Description of Revision Implementation
Replace Figures B-40 and B-41 with updated curve fits for heat A1195-1 (HSST-02).	Reference 1.	The figures being replaced incorrectly showed this material as being LT. The new figures correctly identify the specimens as TL. There are no changes in the tanh fit values/results.
APPENDIX C, CVN FRACTURE APPEARANCE PHOTOGRAPHS		No revisions.
APPENDIX D, DOSIMETER ANALYSIS		No revisions.

Export Control Restrictions

Access to and use of EPRI Intellectual Property is granted with the specific understanding and requirement that responsibility for ensuring full compliance with all applicable U.S. and foreign export laws and regulations is being undertaken by you and your company. This includes an obligation to ensure that any individual receiving access hereunder who is not a U.S. citizen or permanent U.S. resident is permitted access under applicable U.S. and foreign export laws and regulations. In the event you are uncertain whether you or your company may lawfully obtain access to this EPRI Intellectual Property, you acknowledge that it is your obligation to consult with your company's legal counsel to determine whether this access is lawful. Although EPRI may make available on a case-by-case basis an informal assessment of the applicable U.S. export classification for specific EPRI Intellectual Property, you and your company acknowledge that this assessment is solely for informational purposes and not for reliance purposes. You and your company acknowledge that it is still the obligation of you and your company to make your own assessment of the applicable U.S. export classification and ensure compliance accordingly. You and your company understand and acknowledge your obligations to make a prompt report to EPRI and the appropriate authorities regarding any access to or use of EPRI Intellectual Property hereunder that may be in violation of applicable U.S. or foreign export laws or regulations.

The Electric Power Research Institute (EPRI), with major locations in Palo Alto, California; Charlotte, North Carolina; and Knoxville, Tennessee, was established in 1973 as an independent, nonprofit center for public interest energy and environmental research. EPRI brings together members, participants, the Institute's scientists and engineers, and other leading experts to work collaboratively on solutions to the challenges of electric power. These solutions span nearly every area of electricity generation, delivery, and use, including health, safety, and environment. EPRI's members represent over 90% of the electricity generated in the United States. International participation represents nearly 15% of EPRI's total research, development, and demonstration program.

Together...Shaping the Future of Electricity

Program:

Nuclear Power

© 2007 Electric Power Research Institute (EPRI), Inc. All rights reserved. Electric Power Research Institute, EPRI, and TOGETHER...SHAPING THE FUTURE OF ELECTRICITY are registered service marks of the Electric Power Research Institute, Inc.

Printed on recycled paper in the United States of America

1015001NP

Electric Power Research Institute
3420 Hillview Avenue, Palo Alto, California 94304-1338 • PO Box 10412, Palo Alto, California 94303-0813 USA
800.313.3774 • 650.855.2121 • askepri@epri.com • www.epri.com